Molecular Biology of the Cell
Vol. 20, 658–672, January 15, 2009

Role of an Ancestral D-Bifunctional Protein Containing Two Sterol-Carrier Protein-2 Domains in Lipid Uptake and Trafficking in *Toxoplasma*

Bao Lige,* Bamini Jayabalasingham,* Hui Zhang,* Marc Pypaert,† and Isabelle Coppens*

*Department of Molecular Microbiology and Immunology, Johns Hopkins University School of Public Health, Baltimore, MD 21205; and †Department of Cell Biology, Yale University School of Medicine, New Haven, CT 06520

Submitted May 14, 2008; Revised November 3, 2008; Accepted November 4, 2008
Monitoring Editor: Howard Riezman

The inability to synthesize cholesterol is universal among protozoa. The intracellular pathogen *Toxoplasma* depends on host lipoprotein-derived cholesterol to replicate in mammalian cells. Mechanisms of cholesterol trafficking in this parasite must be important for delivery to proper organelles. We characterized a unique D-bifunctional protein variant expressed by *Toxoplasma* consisting of one N-terminal D-3-hydroxyacyl-CoA dehydrogenase domain fused to two tandem sterol carrier protein-2 (SCP-2) domains. This multidomain protein undergoes multiple cleavage steps to release free SCP-2. The most C-terminal SCP-2 carries a PTS1 that directs the protein to vesicles before processing. Abrogation of this signal results in SCP-2 accumulation in the cytoplasm. Cholesterol specifically binds to parasite SCP-2 but with 10-fold lower affinity than phosphatidylcholine. In mammalian cells and *Toxoplasma*, the two parasite SCP-2 domains promote the circulation of various lipids between organelles and to the surface. Compared with wild-type parasites, TgHAD-2SCP-2–transfected parasites replicate faster and show enhanced uptake of cholesterol and oleate, which are incorporated into neutral lipids that accumulate at the basal end of *Toxoplasma*. This work provides the first evidence that the lipid transfer capability of an ancestral eukaryotic SCP-2 domain can influence the lipid metabolism of an intracellular pathogen to promote its multiplication in mammalian cells.

INTRODUCTION

Sterols such as cholesterol are essential components of eukaryotic cell membranes required for proper membrane permeability, fluidity, organelle identity, and membrane protein function. Recent work emphasizes the relevance of these lipids to various pathogenic events, e.g., microbe invasion and multiplication in host mammalian cells (Wenk, 2006). *Toxoplasma gondii*, a leading opportunistic parasite in immunosuppressive conditions, contains significant amounts of cholesterol though it lacks the genes for sterol synthesis and modification (Coppens *et al*., 2000). Parasite cholesterol originates from low-density lipoproteins (LDL) that have been internalized into host cell endocytic compartments. The availability of host cholesterol has a direct impact on *Toxoplasma* development inside its parasitophorous vacuole (PV) because LDL deprivation induces parasite encystation, whereas overabundance of these lipoproteins stimulates parasite replication (Nishikawa *et al*., 2005). The dependence on exogenous sources of cholesterol for the proper development of the parasite implies that *Toxoplasma* must have developed mechanisms for acquiring, transporting, and sorting this lipid. We demonstrated that *T. gondii* uses protective mechanisms such as reverse cholesterol transport (Sehgal *et al*., 2005) and cholesterol storage to balance the influx of cholesterol (Nishikawa *et al*., 2005). The existence of machineries that shuttle cholesterol between the parasite plasma membrane and organelles is implied by the observation that cholesterol is compartimentalized within *T. gondii* (Coppens and Joiner, 2003). However, nothing is known about the mechanisms implicated in translocating cholesterol across *Toxoplasma* membranes and maintaining the nonuniform distribution of this lipid among organelles. The unique nature of organelles present in *T. gondii* and the original features in the parasite physiology augur the existence of unusual cholesterol homeostatic pathways.

Cholesterol can desorb from membranes without the assistance of proteins, but this movement is relatively slow compared with rate at which sterols are trafficked between membranes. In general, cholesterol is moved among cellular compartments by a combination of vesicular and nonvesicular pathways (Prinz, 2007). Several proteins have been proposed to contribute to intracellular sterol trafficking and distribution. These include cytosolic sterol transfer proteins that move sterol between membranes and integral membranes proteins that mediate sterol efflux, and perhaps intracellular sterol transfer. Sterol carrier protein-2 (SCP-2), also known

This article was published online ahead of print in *MBC in Press* (http://www.molbiolcell.org/cgi/doi/10.1091/mbc.E08–05–0482) on November 12, 2008.

Address correspondence to: Isabelle Coppens (icoppens@jhsph.edu).

Abbreviations used: DBP, D-bifunctional protein; HFF, human foreskin fibroblast; LDL, low-density lipoprotein; LPDS, lipoprotein-deficient serum; NHF, normal human fibroblast; PC, phosphatidylcholine; p.i., post-infection; PTS1, peroxisomal targeting signal 1; PV, parasitophorous vacuole; SCP-2, sterol carrier protein-2; TLC, thin layer chromatography; ZF, Zellweger syndrome fibroblast.

as nonspecific lipid transfer protein, is a 13.3-kDa protein conserved among bacteria, archea, and eukaryotes (Gallegos *et al*., 2001). 3-D structural analysis of this protein from different species reveals the conservation of a unique fold that forms a hydrophobic tunnel suitable for the binding of various lipids (Dyer *et al*., 2003). Indeed, in vitro studies report the ability of SCP-2 to transfer not only sterols but also phospholipids, fatty acids, and fatty acyl-CoA between membranes. SCP-2 is specifically targeted to peroxisomes via a C-terminal peroxisomal targeting signal 1 (PTS1), where it is likely involved in peroxisomal β-oxidation of fatty acids. Interestingly, SCP-2–deficient mice show accumulation of methyl-branched fatty acids, which suggests also a physiological role for SCP-2 in α-fatty acid oxidation (Mukherji *et al*., 2002).

SCP-2 is part of a large family of proteins that comprises several enzymes involved in lipid metabolism. The function of SCP-2 at the C terminus of multidomain proteins is still enigmatic. To gain a wider perspective into the biological significance of conserved SCP-2, we have characterized a unique ancestral variant of the D-bifunctional protein (DBP) expressed in *T. gondii*. Although DBP homologues present in fungi and animals contain the three domains D-3-hydroxyacyl-CoA dehydrogenase, enoyl-CoA hydratase, and SCP-2, *Toxoplasma* DBP consists of one N-terminal D-3-hydroxyacyl-CoA dehydrogenase domain connected to two C-terminal SCP-2 domains (Edqvist and Blomqvist, 2006). The reliance of *T. gondii* on host cholesterol for growth implies that the parasite must be proficient at moving this lipid from its surface to intracellular compartments. *Toxoplasma* is incompetent to internalize exogenous molecules by endocytosis that precludes a role for plasma membrane-derived vesicles in cholesterol internalization. As an alternative mechanism, SCP-2 may contribute to the uptake and intracellular circulation of cholesterol in the parasite.

Our results demonstrate that *T. gondii* DBP undergoes multiple cleavage steps, sequentially releasing the SCP-2 domains from the enzymatic portion. Both *Toxoplasma* SCP-2 domains display selective affinity for lipids, show cytosolic and/or vesicular localization, and enhance lipid uptake and metabolism, suggesting their role in lipid shuttling within the parasite. This work represents the first evidence for the existence of a functional SCP-2 domain in a protozoan parasite.

MATERIALS AND METHODS

Chemicals and Antibody

All chemicals were obtained from Sigma-Aldrich (St. Louis, MO) or Thermo Fisher Scientific (Waltham, MA) unless indicated otherwise. Solvents and standards for chromatography were of the highest analytical grade. Silica gel 60 thin layer chormatography (TLC) plates were from Electron Microscopy Sciences (Gibbstown, NJ). Protease inhibitor cocktail tablets were obtained from Roche Applied Science (Indianapolis, IN). Radiolabeled reagents included: [^{14}C]acetate (specific activity, 56 mCi/mmol), [1-^{14}C]oleic acid (specific activity, 55 mCi/mmol), [1-^{14}C]palmitic acid (specific activity, 55 mCi/mmol), [1,2-^{3}H]cholesterol (specific activity, 48 mCi/mmol) were purchased from GE Healthcare (Little Chalfont, Buckinghamshire, United Kingdom). The fluorescent lipids including 22-(*N*-7-nitrobenz-2-oxa-1,3-diazol-4-yl)amino-23,24-bisnor-5-cholen-3β-ol (NBD-cholesterol), 2-(12-(7nitrobenz-2-oxa-1,3-diazol-4-yl)amino)dodecanoy-l-hexadecanyol-*sn*-glycero-3 phosphocholine (NBD-PC), and 2-(4,4-difluoro-5-(4-phenyl-1,3-butadienyl)-4-bora-3a, 4a-diaza-s-indacene-3-pentanoyl)-1-hexadecanoyl-sn-glycero-3-phosphocholine (BODIPY-phosphatidylcholine) were from Invitrogen (Carlsbad, CA). Phophatidylcholine (PC), phosphatidylserine, phosphatidylinositol, cholesterol, ergosterol, and ceramide were purchased from Avanti Polar Lipids (Alabaster, AL). Primary antibodies used in this study were the commercially available mouse monoclonal antibodies against hemagglutinin (HA) (Roche Applied Science), *myc* (Cell Signaling Technology, Danvers, MA), and green fluorescent protein (GFP) (BD Biosciences, Palo Alto, CA).

Mammalian Cell Lines, Culture Conditions, and Parasite Propagation

Mammalian cell lines used included: primary human foreskin fibroblasts (HFFs), COS-7 cells, normal human fibroblasts (NHFs), the human Zellweger syndrome fibroblasts (ZFs) obtained from the Human Genetic Mutant Cell Repository (GM04340; Camden, NJ) and NIH3T3 mouse fibroblasts stably expressing enhanced EGFP-human catalase (generous gift from Dr. A. Kaasch, Johns Hopkins University) in the presence of 500 μg/ml zeocin. All these cells were grown as monolayers and cultivated in α-minimum essential medium (MEM) supplemented with 10% fetal bovine serum (FBS), 2 mM glutamine, and penicillin/streptomycin (100 U/ml/100 μg/ml) as described previously (Coppens *et al*., 2000). The tachyzoite RH strain of *Toxoplasma gondii* was propagated in vitro by serial passage in HFFs (Roos *et al*., 1994).

Sequence Analysis

Nucleotide and amino acid sequences were searched against the *T. gondii* database (www.toxodb.org) and the National Center for Biotechnology Information database using the BLAST algorithm (Altschul *et al*., 1997). Multiple sequence alignment was created using ClustalW, and the resulting similarities were then visualized by subjecting the alignment to Boxshade (www.ch.embnet.org). Percentage of identity and similarity were calculated using standard tools for sequence analysis from National Center for Biotechnology Information (ncbi.nlm.nih.gov).

Cloning of Full-Length cDNA Encoding TgHAD-2SCP-2

Several sequences for the SCP-2 domain were identified in the genome and expressed sequence tags (ESTs) of the *Toxoplasma* database. The open reading frame (ORF) of *TgHAD-2SCP-2* was amplified from a *T. gondii* sporozoite cDNA library (generously provided by Dr. M. W. White, Montana State University) by the use of the primers *TgHAD-2SCP-2*N and *TgHAD-2SCP-2*C (see Supplemental Table S1 for all the sequences of primers used in this study). Amplified fragments (~1.9 kb) were subcloned into pCR2.1 by using the TOPO-TA cloning protocol (Invitrogen, Carlsbad, CA), and the insertion was confirmed by enzymatic digestion with EcoRI and sequencing. The cDNA sequence of TgHAD-2SCP-2 has been deposited in GenBank under the accession number EU348731.

Recombinant Peptide Expression in Escherichia coli and Affinity Purification

Two plasmids have been engineered to produce recombinant peptides. One corresponds to the second SCP-2 domain or SCP-2b (TgHAD-2SCP-$2_{513\text{-}629}$) used for functional studies, and the other one encompasses the C terminus of the D-3-hydroxyacyl-CoA dehydrogenase domain (HAD) domain and the two SCP-2 domains (TgHAD-2SCP-$2_{296\text{-}629}$; see Supplemental Figure S3) and was used to generate antibodies. The coding sequence corresponding to SCP-2b was PCR-amplified using the primers SCP-2-N1 and SCP-2-C1 (Supplemental Table SI) and directly cloned into the BamHI and HindIII sites of the pQE-30 vector (QIAGEN, Hilden, Germany) to generate N-terminal 6-His tagged fusion protein. The coding sequence corresponding to TgHAD-2SCP-$2_{296\text{-}629}$ was polymerase chain reaction (PCR)-amplified using the primers SCP-2-N2 and SCP-2-C1 (Supplemental Table SI) and cloned into the SacI and HindIII sites of the above-mentioned vector to produce an N-terminal 6-His–tagged fusion protein. The recombinant peptides expressed in *E. coli* M15 strain were purified under denatured condition on Ni^{2+}-nitrilotriacetic acid resin according to the QIAGEN protocol. After purification, the peptides were refolded by diluting the sample 10 times in the refolding buffer (50 mM Tris-HCl, pH 7.5, 1 mM EDTA, 1 M L-arginine, 1 mM reduced form of glutathione, and 0.8 mM oxidized form of glutathione) at 4°C overnight. The samples were then concentrated and dialyzed against phosphate-buffered saline (PBS).

Plasmid Construction for Expression in Toxoplasma

Several plasmids were engineered for functional and localization studies of TgHAD-2SCP-2. To generate *T. gondii* stably expressing exogenous copies of TgHAD-2SCP-2, two different plasmids were constructed based on two *T. gondii* expression vectors: sagCATsag_Tub2358YFP and pTub-GFP obtained from the Roos laboratory (University of Pennsylvania). Both vectors facilitate the expression of recombinant proteins in *T. gondii* driven by the tubulin promoter, either with a C-terminal yellow fluorescent protein (YFP) fusion or with an N-terminal green fluorescent protein (GFP) fusion. The plasmid p1HA-TgHAD-2SCP-2 was based on psagCATsag_Tub2358YFP. To construct p1HA-TgHAD-2SCP-2, the TgHAD-2SCP-2 sequence was modified by PCR using primers HA-HAD-2SCP-2-N1 and HA-HAD-2SCP-2-C1 resulting in a fusion protein with the HA tag at the N-terminus. In this construct, a stop codon in the reverse primer was introduced before the YFP coding sequence. The sequence was ligated through BglII and AvrII in the expression vector. The plasmid psagCATsag_Tub2358YFP was also used for the construction of pTgHAD-2SCP-2-YFP to express the chimeric protein TgHAD-2SCP-2-YFP. The primers used for the PCR modification were HAD-2SCP-2-YFP-N and HAD-2SCP-2-YFP-C, which allows the ligation of the sequence between

BglII and AvrII. To obtain the chimeric protein GFP-TgHAD-2SCP-2, the plasmid pGFP-TgHAD-2SCP-2 was produced using the expression plasmid pTub-GFP. For that construct, the 5′ and 3′ ends of TgHAD-2SCP-2 sequence was PCR-modified using the primers HAD-2SCP-2-YFP-N and GFP-HAD-2SCP-2-C and directly ligated to the BglII and AflII sites of pTub-GFP.

Plasmids pHA-SCP-2a, pHA-SCP-2b, and pHA-SCP-2bΔSRL that correspond to N-terminal HA-tagged SCP-2a, SCP-2b, and SCP-2b in which the −SRL motif has been deleted (ΔSRL), were also expressed in *T. gondii*. These plasmids were constructed using the expression vector sagCATsag_Tub2358YFP. PCR were run using the full-length of TgHAD-2SCP-2 as a template and the following primers: HA-SCP-2a-N and HA-SCP-2a-C for pHA-SCP-2a; HA-SCP-2b-N and HA-HAD-2SCP-2-C1 for pHA-SCP-2b; HA-SCP-2b-N and HA-SCP-2bΔSRL-C for pHA-SCP-2bΔSRL. A stop codon was introduced before the YFP coding sequence in the reverse primers. The three PCR products were then digested with BglII and AvrII and ligated to the corresponding sites in sagCATsag_Tub2358YFP. Using the same approach, six plasmids with single amino acid mutations derived from pHA-SCP-2a (pHA-SCP-2a^{M345K}, pHA-SCP-2a^{I433K}, and pHA-SCP-2a^{K434A}) or pHA-SCP-2b (HA-SCP-2b^{M519K}, HA-SCP-2b^{L608K}, and HA-SCP-2b^{K609A}) were engineered using the following primers: HA-SCP-2a^{M345K}-N and HA-SCP-2a-C for pHA-SCP-2a^{M345K}, HA-SCP-2a-N and HA-SCP-2a^{I433K}-C for pHA-SCP-2a^{I433K}, HA-SCP-2a-N and HA-SCP-2a^{K434A}-C for pHA-SCP-2a^{K434A}, HA-SCP-2b^{M519k} and HA-HAD-2SCP-2-C1 for HA-SCP-2b^{M519K}, HA-SCP-2b-N and HA-SCP-2b^{L608K}-C for pHA-SCP-2b^{L608k}, and HA-SCP-2b-N and HA-SCP-2b^{K609A}-C for pHA-SCP-2b^{K609A}.

Expression Analysis in T. gondii and Selection of Parasite Stable Lines

Expression plasmids containing the parasite sequences were grown in *E. coli* DH-5α and isolated using QIAGEN Plasmid Purification kits. Parasites were transfected by electroporation according to a published protocol (Roos *et al*., 1994). For generation of parasites stably expressing tagged versions of TgHAD-2SCP-2 or SCP-2 domains, parasites were transfected, passaged twice in HFF cultures under chloramphenicol selection, and cloned by limiting dilution in 96-well plates.

Plasmid Construction for Expression in Mammalian Cells

Six plasmids were engineered for functional and localization studies of TgHAD-2SCP-2. The pcDNA3.1 vector, which allows the expression of proteins with a *myc*-tag at its C terminus driven by a cytomegalovirus promoter, was used. For the construction of the plasmid p*myc*-TgHAD-2SCP-2, the 5′ and 3′ ends of TgHAD-2SCP-2 were PCR modified using primers *myc*-HAD-2SCP-2-N and SCP-2-C1. The forward primer contains the sequence of *myc*-tag permitting the introduction of the tag at the N terminus of the resulting protein, and the reverse primer contains a stop codon to block the expression of C-terminal *myc*-tag. For pTgHAD-2SCP-2-*myc* engineering, the primers HAD-2SCP-2-*myc*-N and HAD-2SCP-2-*myc*-C were used for PCR modification to generate TgHAD-2SCP-2-*myc*. To construct p*myc*-SCP-2b, which harbors the sequence of SCP-2b with an N-terminal *myc*-tag fusion, primers *myc*-SCP-2-N and SCP-2-C1 were used for the PCR amplification. All three modified PCR fragments were cloned into pcDNA3.1 vector through the EcoRI and HindIII sites.

Three other plasmids, pHA-SCP-2a, pHA-SCP-2b, and pTgHA-SCP-2bΔSRL were engineered similarly to the construction of p*myc*-SCP-2b. Using TgHAD-SCP-2 as the template, SCP-2a or SCP-2b was PCR modified, and the resulting product was directly ligated into EcoRI and HindIII sites of pcDNA3.1. The primers used were SCP-2a-N and SCP-2a-C for pTgHA-SCP-2a, SCP-2b-N and SCP-2-C1 for pTgHA-SCP-2b, and SCP-2b-N and SCP-2bΔSRL-C for pTgHA-SCP-2bΔSRL. The forward primers contain an HA tag coding sequence to result in N-terminal HA-tagged peptides, and the reverse primers contain a stop codon before the restriction site HindIII to block the translation of downstream *myc*-tag sequence.

Expression Analysis in Mammalian Cells and Selection of Stable Cell Lines

Transfection of NIH3T3 cells and COS cells with p*myc*-TgHAD-2SCP-2, pTgHAD-2SCP-2-*myc*, pHA-SCP-2a, pHA-SCP-2b, or pTgHA-SCP-2bΔSRL was completed using lipofectamine method according to the protocol (Invitrogen). For transfection of ZF with p*myc*-SCP-2, both lipofectamine method and human dermal fibroblast nucleofactor kit (Amaxa Biosystems, Gaithersburg, MD) were used, and stable cell line was established by selecting on geneticin (Invitrogen).

Generation of Antibodies against TgHAD-2SCP-2$_{296\text{-}629}$

To monitor TgHAD-2SCP-2 expression, rabbit polyclonal antisera were generated using the His-tagged recombinant TgHAD-2SCP-2$_{296\text{-}629}$ (Covance, Berkeley, CA). Before use, the sera containing antibodies against TgHAD-2SCP-2$_{296\text{-}629}$ (referred as anti-TgHAD-2SCP2 antibodies) were affinity-purified against the recombinant SCP-2b according to the protocol by AminoLink kit (Pierce Chemical).

Immunoblot Analysis of Wild-Type Parasites and Transfectants

For immunodetection, wild-type and transgenic parasites were lysed by suspension in SDS gel-loading buffer (50 mM Tris-HCl, pH 6.8, 50 mM 2-mercaptoethanol, 2% SDS, 0.1% bromphenol blue, and 10% glycerol) followed by boiling in a water bath. The samples were subjected to SDS-polyacrylamide gel electrophoresis (PAGE), and the proteins were then electrophoretically transferred to a membrane (Immobilon transfer membranes; Millipore, Billerica, MA). The membrane was immersed in blocking buffer (phosphate-buffered saline [PBS] containing 3% skim milk) for 60 min, and then incubated with anti-TgHAD-2SCP-2(1:1000), anti-HA antibody (1:5000) or anti-GFP antibodies (1:1000) in the blocking buffer for 60 min. Unbound antibody was removed by washing the membrane six times with blocking buffer. Next, the membrane was incubated with horseradish peroxidase-conjugated goat anti-mouse immunoglobulin G (IgG) antibody (1:10,000; GE Healthcare) in blocking buffer for an additional hour, before detection by chemiluminescence using ECL-Plus (GE Healthcare).

Preparation and Treatment of Crude Vesicle Preparations Containing TgHAD-2SCP-2

T. gondii expressing HA-TgHAD-2SCP-2 (freshly lysed out of host cells) were filtered through 3-μm filter and collected by centrifugation at 1300 × *g* for 10 min at 4°C. After washing in PBS, transfectants (10^9 parasites) were then homogenized before low-speed centrifugation to eliminate large debris as described previously (Bradley *et al*., 2005). The supernatant was centrifuged at 50,000 × *g* for 90 min to obtain a high-speed organellar pellet. After extensive washing of the pellet, a fraction was mixed with protease inhibitors (1 mM EDTA; Complete protease inhibitor mixture), whereas another fraction was first treated with proteinase K (final concentration, 300 μg/ml) for 30 min at 4°C and then with phenylmethanesulfonyl fluoride (final concentration, 500 μg/ml). After these treatments, proteins from these fractions were precipitated with trichloroacetic acid and subjected to Western blotting analysis using anti-TgHAD-2SCP-2 and anti-HA antibodies.

NBD-labeled Lipid Binding to SCP-2

NBD-labeled cholesterol or NBD-labeled PC were selected to determine the interaction of those lipids with recombinant SCP-2b as described previously (Avdulov *et al*., 1999). Briefly, 0.2 μl of NBD-labeled lipids (1×10^{-3} M cholesterol or 1×10^{-4} M PC dissolved in dimethylformamide) was repeatedly added to 1 ml of sample buffer (PBS, in the presence or the absence of 1 μl of 6.7×10^{-7} M of SCP-2b) and stirred for 3 min before excitation at 460 nm and measurement of fluorescence intensity emitted at 550 nm by using a PerkinElmer fluorescence instrument (PerkinElmer Life and Analytical Sciences, Boston, MA). Scatchard plot was used to determine the K_d and B_{max} values of these lipids to SCP-2b.

Spectrofluoremetric Assay to Monitor SCP-2b-mediated PC Transfer Activity

A fluorescence-based direct binding assay was used for measuring the transfer of PC between two bilayer vesicle populations in the presence of SCP-2b. Practically, small unilamellar bovine brain sphingomyelin/cholesterol mixed (6:1) acceptor vesicles or donor vesicles containing BODIPY-PC were prepared by probe sonication as described previously (Mattjus *et al*., 1999; Edqvist *et al*., 2004). Equal volume of donor vesicles and acceptor vesicles were vortexed, resulting in final phospholipid concentrations of 0.025 and 0.25 mM for the donor and acceptor, respectively.

To identify potential substrates for SCP-2b, competition assays were performed using unlabeled lipids and BODIPY-PC incorporated into donor vesicles. The efficiency of competition was determined by measuring the decrease in BODIPY fluorescence emission. These fluorescence dequenching assays started by addition of 1 μg of SCP-2b (0.06 μM) to BODIPY-PC incorporated into liposomes as described above, and after a steady transfer rate was reached, 2 μg of competing unlabeled lipids was added as liposomes to the reaction mixture as described previously (Edqvist *et al*., 2004). After correction for direct excitation of BODIPY in the absence of protein, the decrease in fluorescence emission was normalized relative to the decrease observed with liposomes without competitor. The displacement of BODIPY from SCP-2 by competing lipid substrates was analyzed by fitting the normalized fluorescence decrease to a hyperbolic function.

Cell Surface Transport Assay of Newly Synthesized Cholesterol

Confluent transfected ZFs and COS cells were incubated in MEM containing 10% lipoprotein-deficient serum (LPDS; prepared as described in Coppens *et al*., 2000) for 48 and 24h, respectively. After 24 h, COS cells were transiently transfected with *myc*-TgHAD-2SCP-2, HA-TgSCP-2a, HA-TgSCP-2b, or HA-TgSCP-2bΔSRL and maintained for one additional day in MEM plus 10% LPDS. On day 3, cells were pulsed with 20 μCi of [^{14}C]acetate in ethanol (<1% final concentration) for 7 min at 37°C. The medium was removed and the label was chased by the addition of MEM containing 10 mM sodium acetate for the

indicated chase times. Cells were then washed twice in the assay buffer (310 mM sucrose, 1 mM $MgSO_4$, and 0.5 mM sodium phosphate, pH 7.4) at 25°C. Cholesterol oxidase (0.5 IU/ml) was added in the assay buffer, and the cells were incubated for 3 min at 25°C in conditions described previously (Brasaemle and Attie, 1990). The assay buffer was removed, and the cells were immediately extracted with chloroform:methanol (2:1). The chloroform phase was dried under nitrogen, resuspended with chloroform:methanol (1:1), and applied together with standards to a TLC plate. Plates were developed in hexane:ethyl ether:acetic acid (87:20:1) and visualized with iodine vapor. Spots were scraped and counted in a liquid scintillation counter. In a separate set of experiments, NHFs, transfected ZFs, and transfected COS cells were exposed 30 μCi of [^{14}C]acetate for 7 min at 37°C to monitor cholesterol synthesis compared with mock-transfected ZF and mock-transfected COS cells. After the pulse, cells were incubated for 10, 20, 30, 40, and 60-min in the chase medium before washing. Lipids were extracted for total radioactive cholesterol recovery by TLC by using the solvent described above.

Lipid Uptake and Incorporation Assays in Mammalian Cells

For lipid uptake assays, confluent control ZF, SCP-2b–expressing ZFs, control COS cells, and COS cells expressing TgHAD-2SCP-2 or TgSCP-2bΔSRL were incubated in MEM with 10% FBS containing either 5 μCi of [^{14}C]oleate conjugated to bovine serum albumin (BSA) or 30 μCi [^{3}H]cholesterol incorporated into LDLs (prepared as described in Coppens *et al*., 1995) for 3 h at 37°C. Cells were then washed at 4°C, twice with PBS-Ca^{2+} (137 mM NaCl, 5.4 mM KCl, 0.34 mM Na_2HPO_4, 0.44 mM KH_2PO_4, 3.6 mM $CaCl_2$, and 0.8 mM $MgSO_4$, at pH 7.4) containing 1% (wt/vol) BSA and then twice with PBS-Ca^{2+} alone. Washed cells were lysed in 1 ml of 1% (wt/vol) sodium deoxycholate, pH 11.3, for protein content and radioactivity determination. For assays of oleate metabolism, cells were incubated in MEM with 10% FBS containing 25 μCi of [^{14}C]oleate-BSA for 20-min at 37°C, then washed as described above. After lipid extraction in chloroform:methanol (2:1), the chloroform layer was separated from the aqueous layer by centrifugation, evaporated under nitrogen, and either resuspended in chloroform:methanol (2:1) for phospholipid recovery (PC and phosphatidylethanolamine) followed by TLC chromatography using chloroform:methanol:water (100:42:6), or resuspended in chloroform for triacylglycerol (TAG) and cholesteryl ester separation by TLC chromatography using petroleum ether:diethyl ether:acetic acid (80:20:1) as solvent. Bands were cut, and their radioactivity was measured by liquid scintillation counting.

Lipid Uptake and Incorporation Assays in T. gondii

For lipid uptake assays, HFFs were infected with control parasites or *T. gondii* expressing HA-TgSCP-2a, HA-TgSCP2-b, HA-TgSCP-2bΔSRL, HA-TgSCP-2a^{M345K}, HA-TgSCP-2b^{M5195K}, HA-TgSCP-2a^{I433K}, HA-TgSCP-2b^{L608K}, HA-TgSCP-2a^{K434A},or HA-TgSCP-2b^{K609A} for 48 h before incubation in MEM with 10% FBS containing 15 μCi of [^{14}C]oleate-BSA (C18:1), 15 μCi of [^{14}C]palmitate-BSA (C16:0), or 30 μCi of [^{3}H]cholesterol-LDL for 6 h at 37°C. After washing, intracellular parasites were purified by density gradient using Nycodenz and isopycnic centrifugation as detailed previously (Coppens *et al*., 2000). Amounts of cell-associated lipids were determined by radioactivity and normalized by parasite protein content. For fatty acid incorporation assays, infected HFF were incubated in MEM with 10% FBS containing 35 μCi of [^{14}C]oleate-BSA or of [^{14}C]palmitate-BSA for 60 min. After washing and parasite isolation, protein concentration was determined on an aliquot, before lipid extraction and separation by TLC as described above.

Light and Electron Microscopy Studies

Light and epifluorescence microscopy were performed on infected cells seeded on sterile coverslips in 24-well culture dishes. Immunofluorescence assay (IFA) on parasites or mammalian cells were performed as described previously (Coppens and Joiner, 2003) by using as primary antibodies affinity-purified anti-TgHAD-2SCP-2 (1:100), anti-*myc* (1:100), anti-HA (1:1000), or anti-GFP (1:200), and as secondary antibodies (Invitrogen) anti-mouse and anti-rabbit IgG conjugated to either Alexa 488 or Alexa 594 before dilution at 1:2000. For detection of cholesterol or lipid bodies by fluorescence microscopy, intravacuolar parasites were fixed in paraformaldehyde, and treated as described previously (Coppens and Joiner, 2003; Quittnat *et al*., 2004). Slides were observed using a Nikon Eclipse E800 microscope equipped with a Spot RT charge-coupled device camera and processed using Image-ProPlus software (Media Cybernetics, Silver Spring, MD) before assembly using Adobe Photoshop (Adobe Systems, Mountain View, CA). For immunoelectron microscopy, *Toxoplasma*-infected cells were fixed in 4% paraformaldehyde (Electron Microscopy Sciences, Hatfield, PA) in 0.25 M HEPES, pH 7.4, for 1 h at room temperature, and then in 8% paraformaldehyde in the same buffer overnight at 4°C. They were infiltrated, frozen, and sectioned as described previously (Nishikawa *et al*., 2005). The sections were immunolabeled with anti-TgHAD-2SCP-2 antibodies (1:20 in PBS/1% fish skin gelatin) and then with mouse anti-rabbit IgG antibodies, followed directly by 10-nm protein A-gold particles (Department of Cell Biology, Medical School, Utrecht University, Utrecht, The Netherlands) before examination with a Philips CM120 electron microscope (Eindhoven, The Netherlands) under 80 kV.

Protein Determination

Protein content was determined using the bicinchoninic acid assay (Smith *et al*., 1985) with BSA as a standard.

Statistical Analysis

For comparison of means, p was determined using analysis of variance against control (ANOVA 2).

RESULTS

Molecular Characterization of an Ancestral DBP in T. gondii

In a search for SCP-2-like domains, one gene coding for a peroxisomal multifunctional enzyme type 2 was identified in the *Toxoplasma gondii* genome (46.m01618). Phylogenetic analysis on the evolutionary history of SCP-2 gene fusions revealed that this gene from *T. gondii* was a variant of DBP encoding one N-terminal HAD connected to two C-terminal SCP-2 domains (Edqvist and Blomqvist, 2006). We named this multidomain protein TgHAD-2SCP-2. In contrast to many organisms in which the SCP-2 domain is also expressed from a unique gene, no gene coding for SCP-2 alone was detected in *T. gondii*.

The ORF of *TgHAD-2SCP-2* was amplified by PCR from a sporozoite cDNA library and also by RT-PCR from tachyzoite total RNA (Supplemental Figure S1). The ORF is 1887 nucleotides, consists of nine exons, and encodes a polypeptide of 629 amino acids, with a predicted mass of 67.9 kDa. Located at the N terminus, the HAD domain contains 321 amino acids (predicted size, 35 kDa) and shares 51% identity and 71% similarity with the sequence of the human HAD domain present in DBP (see HAD alignment in Supplemental Figure S2). The first SCP-2 domain (SCP-2a, extending from amino acid 322-448; predicted size of 13-kDa) is directly connected to HAD and is separated from the second SCP-2 domain (SCP-2b, extending from amino acid 513-629; predicted size of 13-kDa) by 61 amino acids. SCP-2a and SCP-2b are 36% identical and 58% similar to each other. Essential amino acids for the sterol transfer function are conserved in both SCP-2 domains (Figure 1A–B). Accordingly, tertiary structural analysis of the parasite SCP-2 domains by using Swiss-Prot software suggests that their core may also form a hydrophobic cavity through five-stranded β-sheets on one side covered by five α-helices (Choinowski *et al*., 2000). The three C-terminal residues of SCP-2b, a tripeptide consisting of −SRL, suggest the presence of a putative PTS1 (Keller *et al*., 1991).

Analysis of the deduced amino acid sequence of the *Toxoplasma* SCP-2 domains revealed their similarity to members of the SCP-2 protein family (Figure 1B). SCP-2a has 33% identity and 58% similarity with human SCP-2 and 36% identity and 57% similarity with *Arabidopsis* SCP-2. By comparison, SCP-2b is 40% identical and 60% similar to human SCP-2 and 47% identical and 69% similar with plant SCP-2.

TgHAD-2SCP-2 Undergoes Multiple Processing Steps

In mammalian cells, fusion proteins carrying a SCP-2 domain are posttranslationally cleaved between the enzymatic portion and the SCP-2 domain (Gallegos *et al*., 2001). To determine whether TgHAD-2SCP-2 is cleaved to release SCP-2a and/or SCP-2b, lysates of wild-type parasites were analyzed by Western blotting using antibodies against the TgHAD-2SCP-$2_{296-629}$ sequence (Figure 2). Data revealed three bands on immunoblots. The highest band, at 69 kDa (band A) and the lowest band at 13 kDa

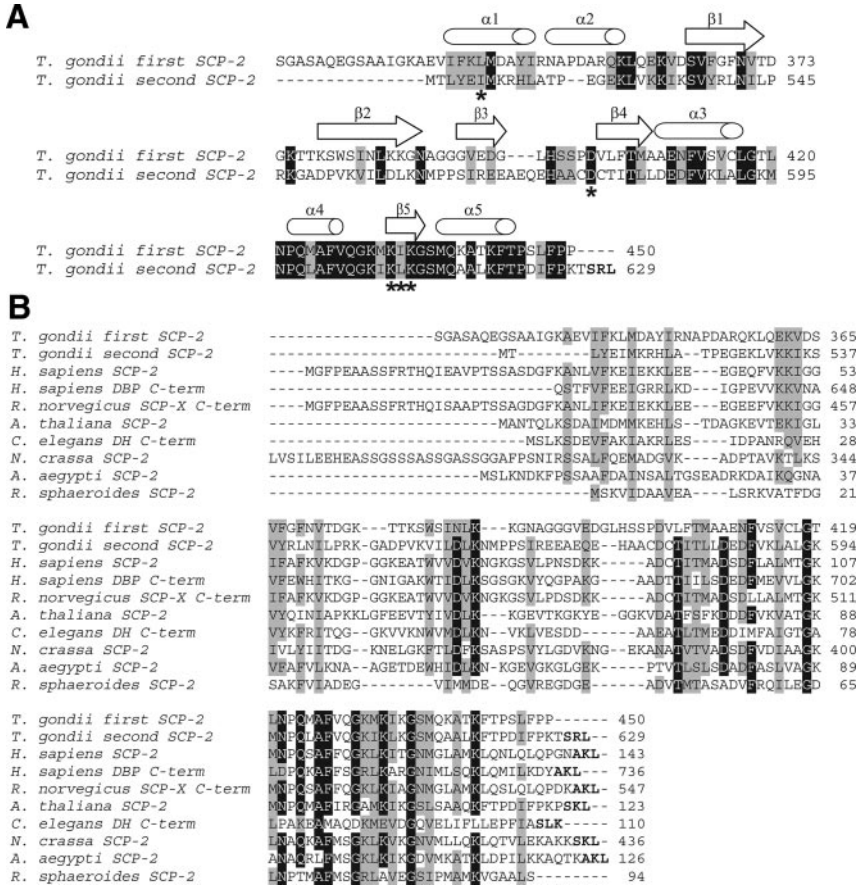

Figure 1. Sequence alignment of the predicted sequences of the SCP-2 domains of *T. gondii* and comparison with other organisms. (A) Sequence alignment of the two parasite SCP-2 domains by using the CLUSTALW program. Black and gray boxes indicate identical and similar amino acids, respectively. Amino acids in bold highlight the PTS1. Stars show residues that are important for the sterol transfer function (Stolowich *et al.*, 2002). α1–5, α-helices 1–5; β1–5; β-sheets 1–5. (B) Multiple sequence alignment of individual *T. gondii* SCP-2 domain with the sequences from *Homo sapiens* SCP-2 (AAA03559), human SCP-2 domain at the C terminus of the DBP (P51659), *Rattus norvegicus* (P11915), *Arabidopsis thaliana* SCP-2 (NP_199103), *Aedes aegypti* (AAQ08007), *Caenorhabditis elegans* SCP-2 domain at the C terminus of the short chain dehydrogenase (AAK68187), *Neurospora crassa* SCP-2 (XP_960876), and *Rhodobacter sphaeroides* SCP-2 (YP_352482).

(band D), correspond to the predicted sizes of the full-length protein and separate SCP-2 domain, respectively. We hypothesize that the 36-kDa intermediate band (band B) represented either the HAD domain alone or SCP-2a still fused to SCP2b. To discriminate between these possibilities, we engineered a tagged version of TgHAD-2SCP-2. *TgHAD-2SCP-2* was cloned from cDNA into a *T. gondii* expression vector and a HA tag was inserted at the N terminus (p1HA-TgHAD-2SCP-2). This construct was transfected into tachyzoites and stably integrated to generate the strain HA-TgHAD-2SCP-2 for Western blotting analysis. A major 70-kDa protein, corresponding to the predicted size of HA-tagged-TgHAD-2SCP-2 was recognized in this strain using either antibodies against TgHAD-2SCP-2$_{296\text{-}629}$ or HA (Figure 2, b and c, band

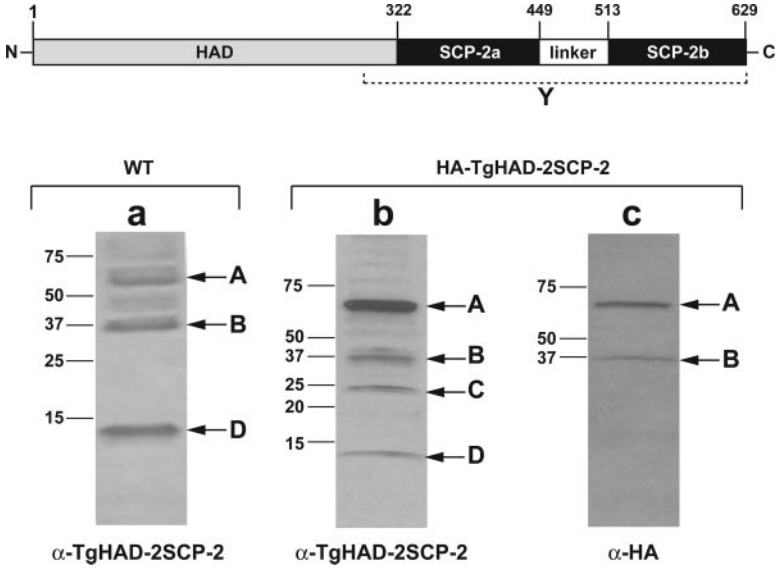

Figure 2. Posttranslational modification of TgHAD-2SCP-2 in wild-type *T. gondii* and transgenic parasites expressing HA-TgHAD-2SCP-2. Top, schematic representation of TgHAD-2SCP-2 showing the multidomains and their presumed length as indicated by the position of amino acids based on homology with various D-3-hydroxyacyl-CoA dehydrogenase and SCP-2 primary sequences. The dashed line and oversized Y indicate the antigenic fragment used to produce the anti-TgHAD-2SCP-2 antiserum. a–c, immunoblots of wild-type *T. gondii* (a) or parasites transfected with p1HA-TgHAD-2SCP-2 (b and c). Western blots analyses of the gel were probed with anti-TgHAD-2SCP-2 (a and b) or anti-HA (c) antibodies. The same blot has been used in b and c. Band A represents the full-length protein, whereas bands B, C, and D show fragments that are equivalent for each blot. The molecular weight markers in kilodaltons are at the left margin.

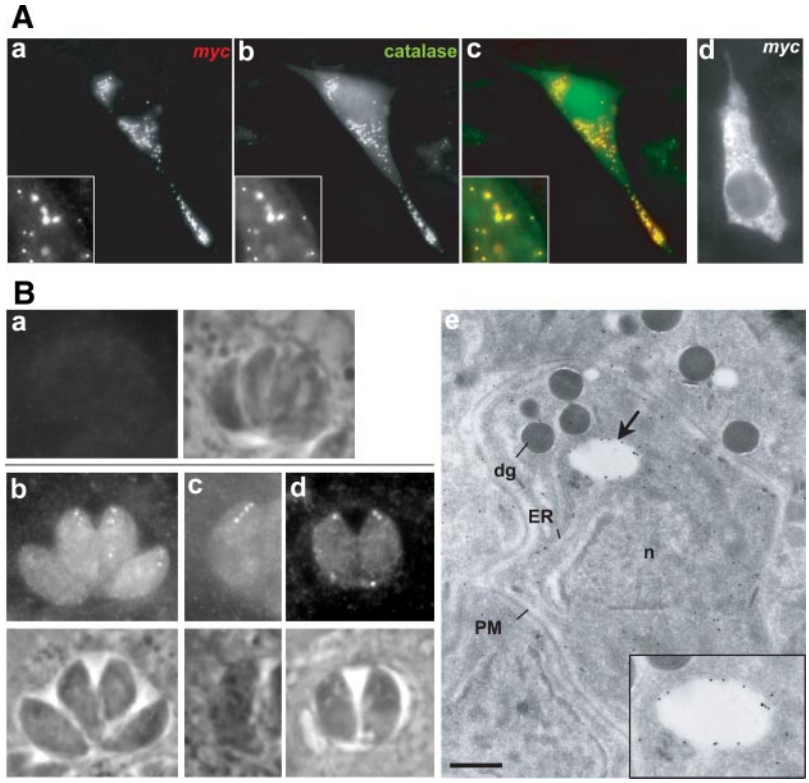

Figure 3. Subcellular distribution of TgHAD-2SCP-2 in wild-type *Toxoplasma* in comparison with mammalian cells transfected with TgHAD-2SCP-2. (A) Fluorescence assays on human fibroblasts stably expressing EGFP-catalase (b) and transfected with p*myc*-TgHAD-2SCP-2 (a) or pTgHAD-2SCP-2-*myc* (d) before labeling with anti-*myc* antibodies. (B) a–d, IFA on wild-type intracellular parasites labeled with preimmune serum (a) or anti-TgHAD-2SCP-2 (b–d). e, immuno-EM labeling on cryosections of *Toxoplasma*-infected fibroblasts using anti-TgHAD-2SCP-2 antibodies revealing the morphology of a TgHAD-2SCP-2-containing vesicle (arrow). dg, secretory dense granule; n, nucleus; PM, plasma membrane. Bar, 0.5 μm.

A). In addition, three minor bands at 37, 23, and 13 kDa could be generally detected using anti-TgHAD-2SCP-2 antibodies (Figure 2b, bands B–D), suggesting that the full-length 69-kDa protein is processed to generate three fragments. Using anti-HA antibodies against HA-TgHAD-2SCP-2 lysate (Figure 2c), we determined that the 37-kDa band corresponded to the HAD domain and that the 13-kDa band was likely SCP-2b. No 23-kDa band was identified using anti-HA antibodies, indicating that this band corresponds to SCP-2a fused to the linker region. Together, these observations suggest that TgHAD-2SCP-2 undergoes at least two processing steps that occur simultaneously. Indeed, no band corresponding to HAD connected to SCP-2a (expected size, 55-kDa) has been detected in our experiments. Further processing, e.g., trimming of the linker from SCP-2a, cannot be excluded. The absence of the 23-kDa band in wild-type parasites may be due to the rapid processing of SCP-2a after the removal of the linker, or alternatively overexpression of the protein may slow the posttranslational processing, allowing the visualization of intermediate cleavage products in HA-TgHAD-2SCP-2–expressing cells. When TgHAD-2SCP-2 was tagged with N-terminal GFP, only a single band at 100-kDa corresponding to uncleaved GFP-TgHAD-2SCP-2 was detected with anti-GFP antibodies (data not shown). This observation indicates that the N-terminal GFP tag likely interferes with posttranslational folding and processing of TgHAD-2SCP-2.

TgHAD-2SCP-2 Localizes to Peroxisomes in Mammalian Cells

So far, catalase is the only example of a *Toxoplasma* protein that harbors a putative PTS1 (-AKM; Kaasch and Joiner, 2000; Ding *et al*., 2000). The peroxisome targeting potential of the C-terminal −SRL motif of TgHAD-2SCP-2 was probed by expressing TgHAD-2SCP-2 with a N-terminal *myc* tag in fibroblasts expressing the peroxisomal protein catalase fused to GFP (Figure 3A, a–c). These experiments revealed a superimposable punctate pattern of TgHAD-2SCP-2 and catalase within the same cell, implying that the parasite protein localizes to mammalian peroxisomes. Control experiments were performed using a plasmid in which PTS1 was masked by the addition of a C-terminal *myc* tag (pTgHAD-2SCP-2-*myc*). In this case, the parasite protein yielded a staining spread through the cell (Figure 3Ad), which is consistent with a predicted endoplasmic reticulum (ER) and cytosolic localization (Edqvist *et al*., 2004).

TgHAD-2SCP-2 Distributes to Vesicles and Cytosol in Toxoplasma

We next determined the intracellular distribution of TgHAD-2SCP-2 and cleaved products in wild-type *Toxoplasma* by light and electron microscopy (EM) by using anti-TgHAD-2SCP-2 antibodies (Figure 3B and Supplemental Table S2). Wild-type tachyzoites showed labeling in the cytoplasm and in well-defined vesicles preferentially localized at both the parasite extremities. Immuno-EM studies confirmed this staining, and closer examination of immunolabeled vesicles revealed that gold particles were bound to a limiting membrane, predominantly on the luminal side. The shape of the vesicles containing TgHAD-2SCP-2 and/or its processed products varied from spherical to oval with a mean diameter of 450 nm and an electron-lucent matrix. In mammalian cells, SCP-2 is localized to peroxisomes, and also to the ER and mitochondria (Gallegos *et al*., 2001). By comparison, no significant labeling of TgHAD-2SCP-2 could be detected above background in any other known compartment of *Toxoplasma*.

Our data above indicate that TgHAD-2SCP-2 is cleaved into three products corresponding to the HAD, SCP-2a, and SCP-2b domains. To define the localization of specific do-

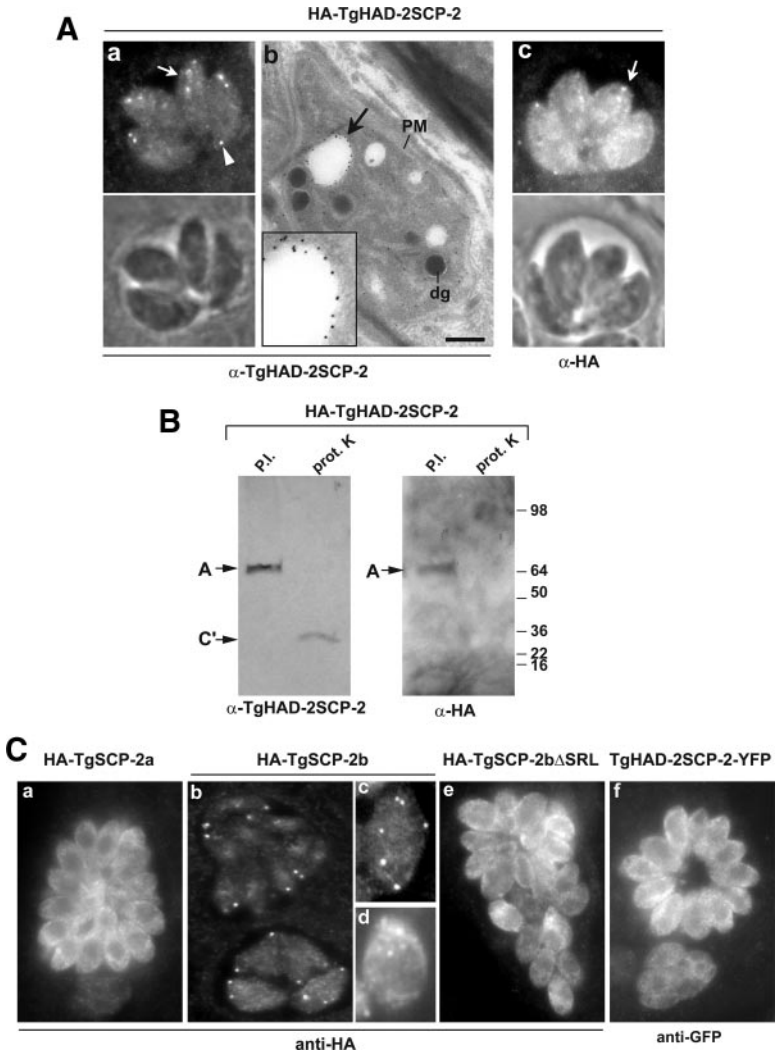

Figure 4. Localization and topology TgHAD-2SCP-2 and its cleavage products in transgenic parasites expressing various constructs derived from TgHAD-2SCP-2. (A) Parasites expressing HA-TgHAD-2SCP-2 labeled with anti-TgHAD-2SCP-2 antibodies for IFA (a) and immuno-EM (b), or with anti-HA antibodies (c). In fluorescence microscopy pictures, arrows and arrowheads show vesicles at the apical and basal ends of the parasite, respectively. In EM pictures, arrows pinpoint TgHAD-2SCP-2-containing structures. dg, secretory dense granule; n, nucleus; PM, plasma membrane. Bar, 0.5 μm. (B) Immunoblot of subcellular fractions of HA-TgHAD-2SCP-2–expressing parasites revealed first with anti-TgHAD-2SCP-2 and then with anti-HA antibodies. After parasite homogenization and clearance of the lysate of debris, the supernatant was collected to isolate vesicles by high-speed centrifugation. Vesicles from the pellet were either treated with protease inhibitors (P.I.) or subjected to mild proteolysis with proteinase K (prot. K) before Western blot analysis. The relative molecular weight of bands A and C′ is 69 and 35 kDa, respectively. The molecular weight markers in kilodaltons are at the right margin. (C) IFA on intracellular parasites stably expressing HA-Tg2SCP-2a, HA-Tg2SCP-2b, HA-Tg2SCP-2bΔSRL, or TgHAD-2SCP-2-YFP revealed by anti-HA antibodies (a–e) or anti-GFP antibodies (f). c and d, magnification of two single parasites that are representative of the dual localization of Tg2SCP-2b in vesicles (c) and in the cytosol (d).

mains, we transfected parasites with various constructs of TgHAD-2SCP-2 in fusion to an epitope tag at either the N terminus or the C terminus. Stable recombinant parasites expressing HA-TgHAD-2SCP-2 were labeled with anti-HA or anti-TgHAD-2SCP-2 antibodies (Figure 4A, a–c). Data illustrated a vesicular and cytosolic pattern, similar to that of wild-type parasites.

To confirm the association of TgHAD-2SCP-2 with vesicles in *T. gondii*, we performed Western blot analysis on pelleted organelles obtained from parasites expressing HA-TgHAD-2SCP-2 using anti-TgHAD-2SCP-2 and anti-HA antibodies on the same blot. A major band corresponding to 69-kDa could be resolved and likely corresponds to the full-length protein (Figure 4B). To determine whether the protein is targeted to the peripheral membrane of vesicles or into the luminal side, we probed the ability of proteases to digest HA-TgHAD-2SCP-2 in isolated intact vesicles. The vesicle-bound HA-TgHAD-2SCP-2 showed partial resistance to proteolysis because a peptide of 35-kDa (band C′) was detected with anti-TgHAD-2SCP-2 antibodies. This result is in accordance with the predominance of TgHAD-SCP-2 on the luminal side of vesicles as seen by immuno-EM (Figures 3Be and 4Ab). The lack of recognition of band C′ band by anti-HA antibodies suggests that the N terminus of TgHAD-2SCP-2 is likely exposed at the surface of the vesicles, and accessible to proteases. Band C′ may then correspond to an internal sequence of HA-TgHAD-2SCP-2 or to the C terminus of the protein.

Next, we wanted to determine whether the C-terminal −SRL motif of SCP-2b functions as a targeting signal for vesicular localization of the protein within the parasite. Parasites stably expressing HA-TgSCP-2a, HA-TgSCP-2b, and HA-TgSCP-2b in which the −SRL motif has been deleted (HA-TgSCP-2bΔSRL) were constructed and stained with anti-HA antibodies for IFA (Figure 4C, a–e, and Supplemental Table S2). When parasites were transfected with HA-TgSCP-2a, the protein was exclusively cytosolic. By comparison, in HA-TgSCP-2b–expressing parasites, immunoreactivity to this domain increased within vesicles over the cytoplasm. This vesicular association was likely due to the −SRL motif because its ablation from TgSCP-2b resulted in cytosol distribution of the truncated domain. Parasites stably expressing TgHAD-2SCP-2 in fusion with YFP at the C terminus (TgHAD-2SCP-2-YFP strain) to abrogate PTS1 function were also tested. Expectedly, the chimeric protein was observed in the cytoplasm (Figure 4Cf). This suggests that, as described for the canonical PTS1 motif on peroxisomal proteins, the position of the −SRL motif at the C terminus of TgHAD-2SCP-2 seems critical to the proper subcellular localization of TgHAD-2SCP-2.

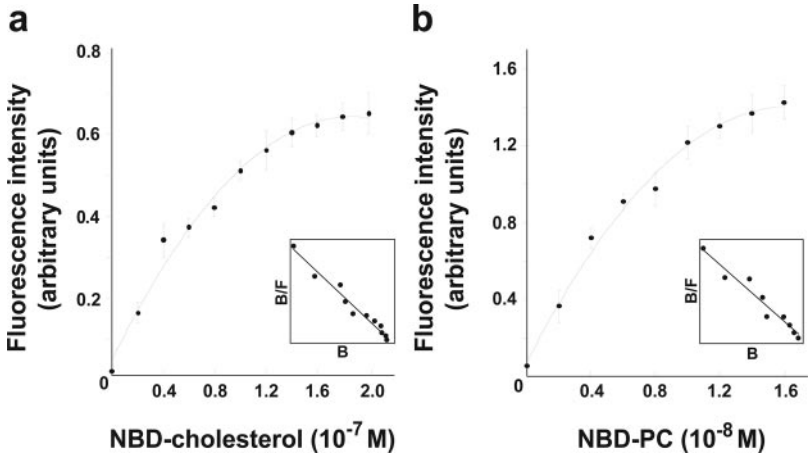

Figure 5. Binding assays of lipids to SCP-2b. Fluorometry assays to monitor the interaction of the recombinant TgSCP-2b with fluorescently labeled lipids at different concentrations. This assay was performed by comparison of the fluorescence intensity in the absence and the presence of the protein. NBD-labeled cholesterol (A) or NBD-labeled PC (B) was incubated with or without SCP-2 (6.7×10^{-7} M) for comparison of fluorescence intensity. Data expressed in arbitrary units, are means ± SD of nine independent assays.

Toxoplasma SCP-2 Binds to Fluorescent Phosphatidylcholine and Cholesterol

Amino acids required for the lipid binding activity of SCP-2 (Stolowich *et al*., 2002) are conserved in both parasite SCP-2 domains (Figure 1A). A fluorescence based direct binding assay was performed to determine the capability of parasite SCP-2 to interact with cholesterol or PC. For this assay, we used an N-terminal His-tagged recombinant peptide corresponding to SCP-2b. Figure 5, A and B, shows titration-binding isotherms for the binding of NDB-cholesterol or NBD-PC to recombinant SCP-2b. Binding curves were saturable in the concentration range analyzed for both lipids. Scatchard plot analyses revealed a fit to a single class of sites (Figure 5, insets), with a K_d value of 1.01 ± 0.12 μM and a B_{max} value of 1.01 ± 0.04 mol/mol for cholesterol and a K_d value of 0.11 ± 0.39 μM and a B_{max} value of 2.45 ± 0.11 mol/mol for PC. Thus, SCP-2b shows lipid binding properties that are typical for this protein and displays the highest affinity for PC.

Toxoplasma SCP-2 Mediates the Transfer of Various Lipids between Membranes

We examined the intermembrane PC transfer capability of SCP-2b (Figure 6). BODIPY-PC was incorporated into donor liposomes, and the transfer of this fluorescent lipid to acceptor liposomes potentially mediated by SCP-2b was measured by fluorospectrometry over a period of time of 16 min. Data showed an increase in BODIPY emission intensity in the presence of SCP-2b as a function of time, reflective of the spatial separation of the BODIPY molecules. This indicates

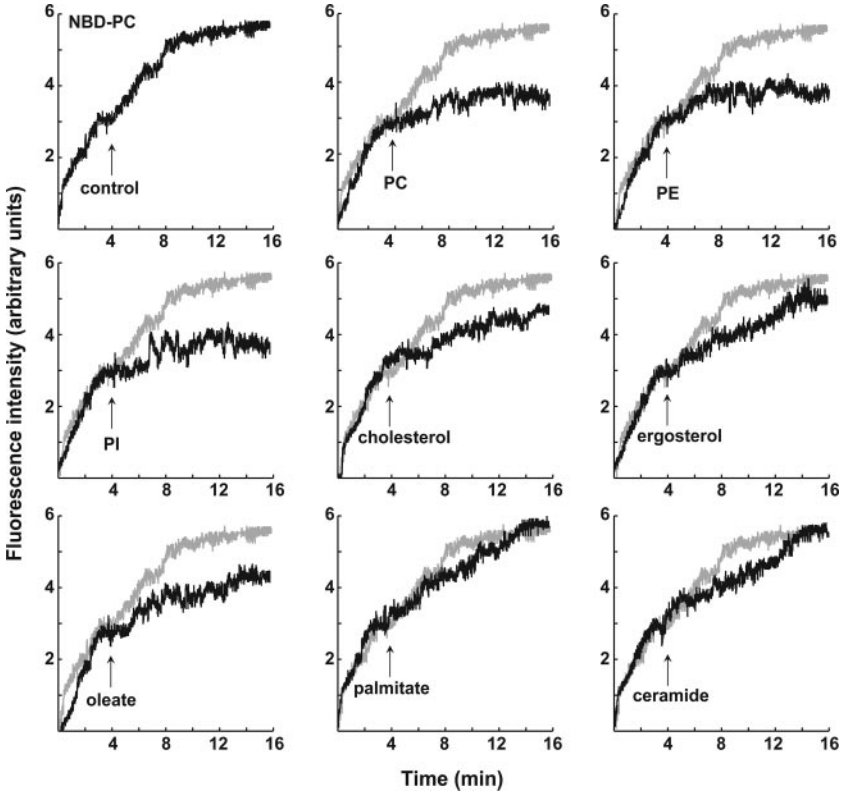

Figure 6. SCP-2b–mediated lipid transfer and competition assays. The intervesicular transfer of BODIPY-PC from donor vesicles to acceptor vesicles was monitored in the presence of SCP-2b. PBS (control) or unlabeled lipids were added to the mixture at the indicated time (arrow), and their plots in black were compared with that of BODIPY-PC without addition of lipids (gray plots). Results shown are representative of three separate experiments. PE, phosphatidylethanolamine; PI, phosphatidylinositol.

that SCP-2b is capable of transferring its substrate PC from one vesicle to another.

To further examine the capability of SCP-2b to mediate the transfer of other lipids, we used competition assays to explore a broad spectrum of lipid substrates (Figure 6). We analyzed the ability of various phospholipids, sterols, fatty acids, and ceramide to compete with BODIPY-PC. SCP-2b was added to the donor liposomes containing BODIPY-PC, and at the steady transfer rate, unlabeled lipids were introduced into the reaction mixture to monitor the transfer rate of BODIPY-PC. Validation of the accuracy of our competition transfer assay was preformed using unlabeled PC, which caused a decrease in the transfer rate of fluorescence. Phosphatidylethanolamine, phosphatidylinositol, cholesterol, and oleate lowered the transfer rate of BODIPY-PC by 20–40%, indicating their ability to displace PC from SCP-2b. Ergosterol showed a marginal competing effect, whereas no deviation in the slope of the transfer rate was observed for palmitate and ceramide. Altogether, these data show that SCP-2b is specialized to transfer a unique subset of lipids compared with other SCP-2 homologues.

Cholesterol Delivery from the ER to the Plasma Membrane Is Accelerated in Zellweger Syndrome Fibroblasts Expressing Parasite SCP-2

A set of experiments was undertaken to investigate the physiological role of TgHAD-2SCP-2 in lipid circulation within cells. A role in cholesterol movement from the ER to the plasma membrane has been ascribed for SCP-2 (Puglielli *et al*., 1995). In ZFs, a cell line deficient in the import of PTS proteins and lacking SCP-2, the transfer of newly synthesized cholesterol to the surface is indeed slower compared with normal cells. We therefore probed the potentiality of parasite TgSCP-2b to accelerate the delivery of endogenous cholesterol to the surface of ZF in comparison with SCP-2 from NHF. Because ZF do not express DBP, we engineered a stable ZF cell line expressing TgSCP-2b (and not TgHAD-2SCP-2), based on the assumption that the machinery for processing the full-length protein may be impaired in ZF. We probed the localization of TgSCP-2b in ZF. ZF have remnant peroxisomes present as membrane ghosts and contain peroxisomal proteins that are mislocalized to the cy-

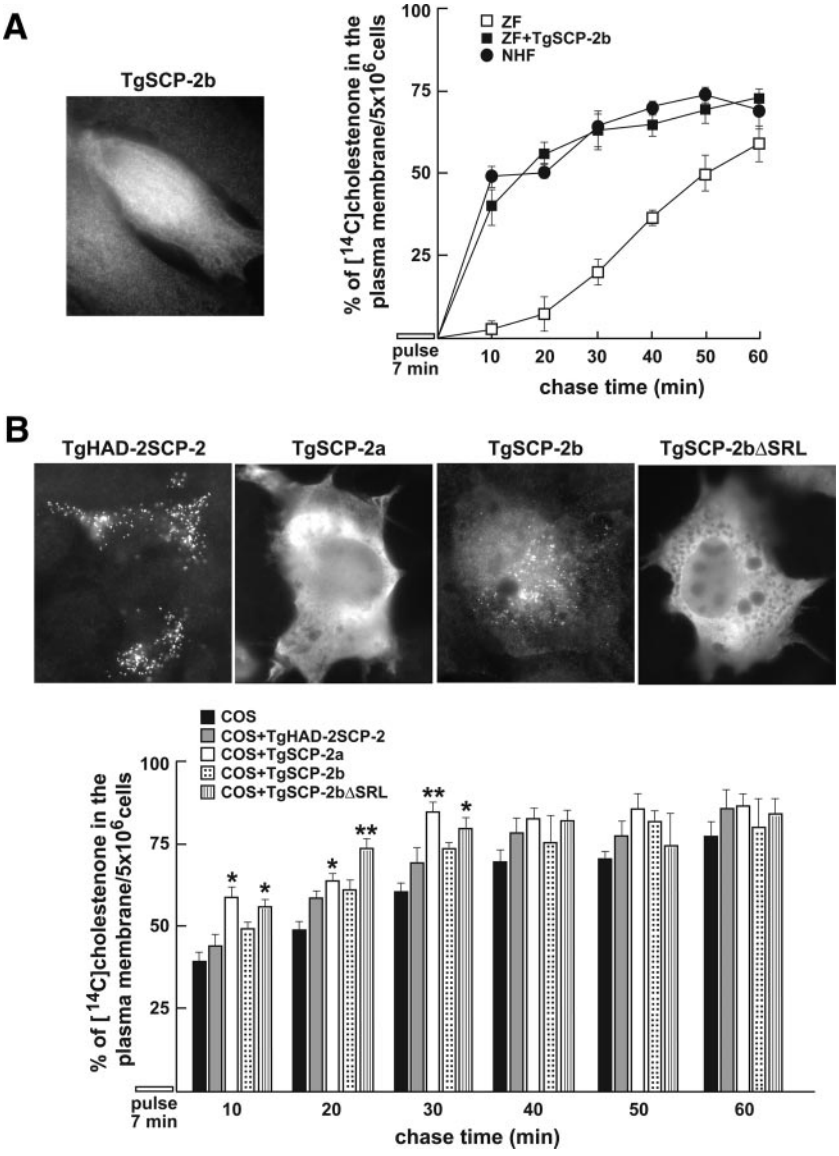

Figure 7. Influence of SCP-2b on transport of newly synthesized cholesterol to the plasma membrane in mammalian cells. (A) Assays on ZF stably expressing *myc*-TgSCP-2b. IFA has been performed on the transfected cells using anti-*myc* antibodies. Confluent ZF controls (mock transfected), transfected with TgSCP-2b, or NHFs) were pulsed with [^{14}C]acetate for 7 min at 37°C and chased for the indicated times. Radioactive cholesterol incorporation in the plasma membrane was determined using the cholesterol oxidase assay. Results are the mean ± SD of three or four experiments and are expressed as percentage of radioactive cholestenone per 5×10^6 cells. (B) Assays on COS cells transiently transfected with plasmids containing *myc*-tagged TgHAD-2SCP-2, HA-tagged TgSCP-2a, HA-tagged TgSCP-2b, or HA-tagged TgSCP-2bΔSRL. IFA performed on the transfected cells with the indicated constructs using anti-*myc* or anti-HA antibodies. The same protocol described in A was used to monitor the cholesterol transfer to the surface of control COS cells (mock transfected), COS cells expressing TgHAD-2SCP-2, TgSCP-2a, TgSCP-2b, or TgSCP-2bΔSRL. Values expressed as indicated in A are means ± SD (n = 3 or 4). *$p < 0.05$ and **$p < 0.01$.

tosol. Expectedly, IFA revealed that TgSCP-2b was localized to the cytoplasm of transfected ZFs (Figure 7A). We used pulse-chase experiments with radioactive acetate to study the rate at which newly synthesized cholesterol occurred at the cell surface. TgSCP-2b–expressing ZFs, untransfected ZF and NHF showed no difference in the amounts and rate of [^{14}C]acetate incorporation into cholesterol, indicative of a comparable rate of cholesterol synthesis (Supplemental Figure S4). The half-times for the appearance of radiolabeled cholesterol at the plasma membrane were 5 and 7 min after the beginning of the pulse in NHF and SCP-2b–expressing ZF, respectively, whereas a value of 35 min was observed for untransfected ZFs under the same conditions.

Identical experiments were conducted on COS cells transiently transfected with a plasmid carrying TgHAD-2SCP-2 or cleaved SCP-2 domains to monitor cholesterol transport to the plasma membrane. In these cells, TgHAD-2SCP-2 seemed to be concentrated in punctate loci, presumably peroxisomes, and to some extent in the cytoplasm (Figure 7B). Expectedly, TgSCP-2a and TgSCP-2bΔSRL showed cytosolic distribution in COS cells, whereas TgSCP-2b localized both to peroxisome-like structures and cytosol. Comparison between transfected COS cells expressing parasite SCP-2 domains and untransfected control cells showed a moderate but significant increase in the kinetics of cholesterol delivery from the ER to the plasma membrane in the cells transfected with TgSCP-2a and TgSCP-2bΔSRL, whereas no difference in cholesterol synthesis was observed between transfected and untransfected COS cells (Supplemental Figure S4). These experiments favor a role for the cytosolic forms of the TgSCP-2 domains in facilitating the movement of cholesterol from the interior of the cell to the surface.

Parasite SCP-2 Enhances Lipid Uptake and Synthesis in Mammalian Cells

In mammalian cells, SCP-2 has multiple roles in intracellular lipid diffusion and metabolism (Gallegos *et al*., 2001; Murphy, 2002). To specify the properties of the parasite SCP-2 in modulating cellular lipid levels, transfected ZF expressing SCP-2b and transfected COS cells expressing TgHAD-2SCP-2 or TgSCP-2bΔSRL were incubated in the presence of radiolabeled oleate and cholesterol to monitor the uptake of these lipids (Figure 8A). After 3-h incubation with the radiolabeled compounds, the expression of the parasite SCP-2 in mammalian cells resulted in an increase in [^{14}C]oleate uptake by 40% in ZF and by 45–50% in COS cells compared with their mock transfected controls. The uptake of [^{3}H]cholesterol was comparable in transfected ZF expressing SCP-2b and controls. By contrast, COS cells expressing TgHAD-2SCP-2 or TgSCP-2bΔSRL incorporated 2 to 2.5 times more cholesterol compared with control cells.

We then examined whether SCP-2-mediated enhancement of oleate uptake modifies the targeting of oleate. COS expressing TgHAD-2SCP-2 or TgSCP-2bΔSRL were incubated with radioactive oleate. Separation of phospholipids and esterified neutral lipids from these cells by TLC revealed that oleate was further incorporated into various lipids (Figure 8B). TgHAD-2SCP-2 expression increased the formation of total phospholipids by 2.1-fold, triglycerides by 1.9-fold and cholesteryl oleate by 2.4-fold. Tg2SCP-2bΔSRL expression also resulted in increase in lipid synthesis with values of 2.3-fold for phospholipids, 2.8-fold for triglycerides, and 3.1-fold for cholesteryl oleate.

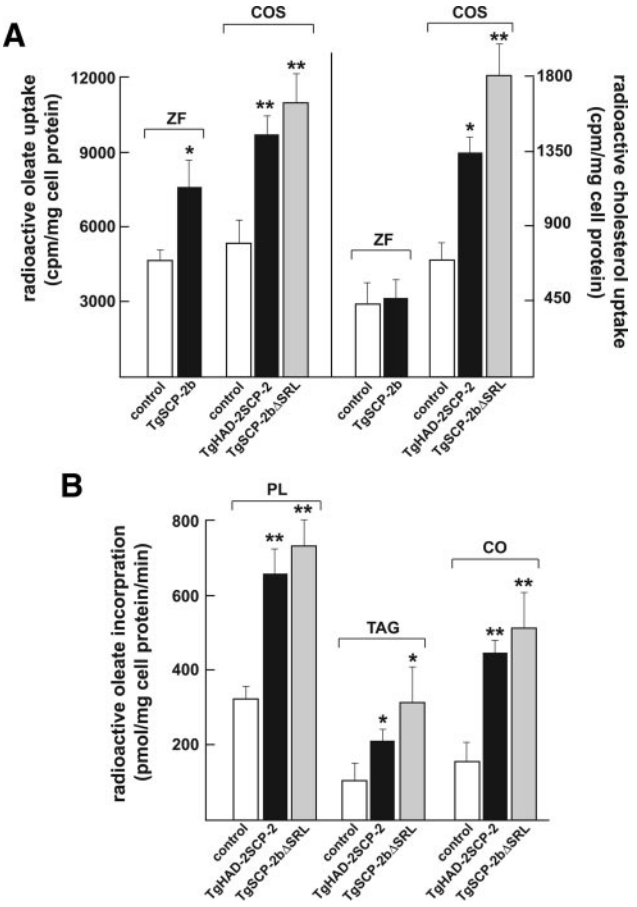

Figure 8. Effect of SCP-2b on fatty acid and cholesterol uptake and incorporation into lipids in mammalian cells. (A) Lipid uptake assays. Confluent control ZF, SCP-2b–expressing ZF, control COS cells, TgHAD-2SCP-2–expressing COS cells, and TgSCP-2ΔSRL-expressing COS cells were incubated with complete MEM containing either [^{14}C]oleate conjugated to BSA or [^{3}H]cholesterol incorporated into LDL for 3 h at 37°C. After washing, the amount of cell-associated lipids was determined by radioactivity and expressed as cpm per milligram of cell protein. Values are means ± SD (n = 3), *$p < 0.05$ and **$p < 0.01$. (B) Lipid incorporation assays. Control COS cells, TgHAD-2SCP-2–expressing COS cells or TgSCP-2bΔSRL–expressing COS were used as described in A except that the incubation time with [^{14}C]oleate-BSA was 20 min. After washing, cell protein concentration was determined, and lipids extracted to quantify the amount of radioactive phospholipids (PL), TAG, and cholesteryl oleate (CO) associated with the cells. Values are means ± SD (n = 3 or 4). *$p < 0.05$ and **$p < 0.01$.

Exogenous Expression of TgHAD-2SCP-2 in Toxoplasma Results in Increased Uptake and Metabolism of SCP-2 Lipid Substrates

Prompted by the observed effects of parasite SCP-2 in mammalian cells, the last series of experiments was focused on the potential of TgHAD-2SCP-2 in regulating lipid transport, synthesis and storage in *T. gondii*. Experiments were performed on parasites expressing HA-TgHAD-2SCP-2 and compared with mock transfected wild-type parasites in a gain-of-function phenotype-driven approach. Parasites were labeled with the fluorescent dye filipin, used for detection of membrane sterols, and HA-TgHAD-2SCP-2 expressors showed a brighter overall fluorescence than wild type (Figure 9A). These parasites were labeled in parallel with Nile red, a fluorescent lipid body dye (Figure 9B). Compared

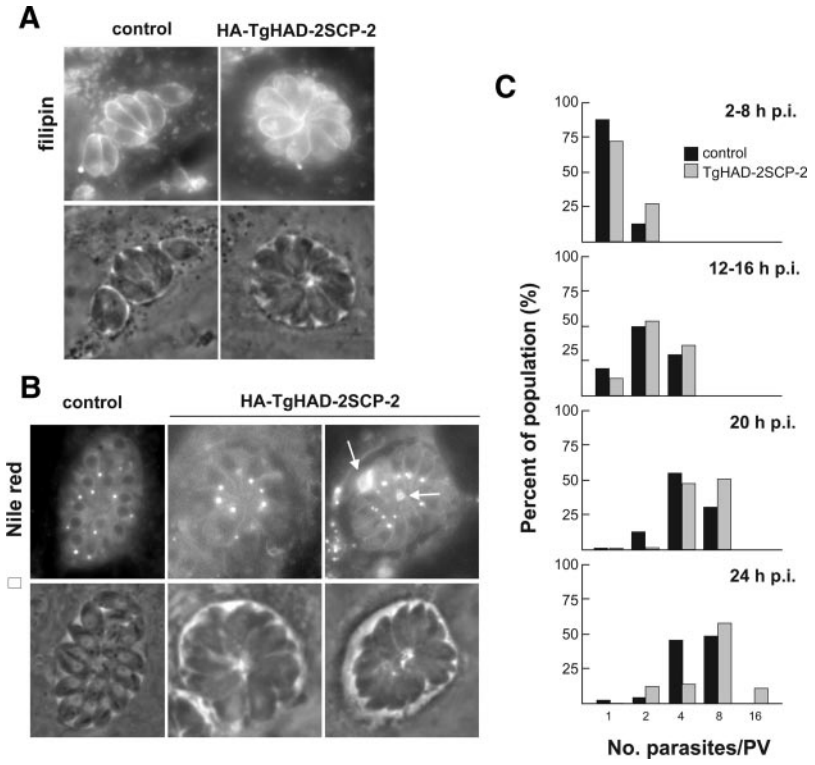

Figure 9. Role of TgHAD-2SCP-2 in lipid distribution and parasite development. (A and B) Fluorescence assays on intracellular parasite either mock transfected as control or stably transfected with HA-TgHAD-2SCP-2. Parasites were incubated with filipin (A) or Nile red (B) to assess the distribution of membrane cholesterol or lipid bodies, respectively. Arrows pinpoint lipids accumulated inside the PV. (C) Quantitative distribution of the number of *Toxoplasma* per PV either wild-type parasites (black) or HA-TgHAD-2SCP-2–expressing parasites (black). Parasite development was monitored at the indicated time points p.i. for two independently infected monolayers.

with control parasites that displayed lipid bodies throughout the cytoplasm without any specific location (Quittnat *et al*., 2004), *T. gondii* expressing HA-TgHAD-2SCP-2 showed an accumulation of lipid bodies at the posterior end, and sometimes in the vacuolar space (Figure 9B, arrows). The concentration of lipid bodies at the basal pole of the parasites where SCP-2 is also accumulated (Figure 4) suggests that this protein plays a role in lipid circulation and association with lipid bodies.

Because *Toxoplasma* growth can be directly dependent upon exogenously supplied lipids (Coppens, 2006), we monitored the replication rate of HA-TgHAD-2SCP-2 expressors compared with wild-type parasites. Results showed that additional copies of TgHAD-2SCP-2 conferred an advantage to parasite growth as measured by enumeration of parasites per PV in infected cells (Figure 9C). Indeed, at 24 h post infection (p.i.), ~10% of the PV from transfectants contained 16 parasites versus <1% among wild-type parasites.

To validate our morphological studies, the uptake of exogenous lipids was then monitored in *Toxoplasma*-infected cells exposed to radiolabeled lipids, followed by parasite purification and radioactivity determination (Figure 10). Data showed that parasites stably expressing HA-TgHAD-2SCP-2 accumulated higher amounts of [^{14}C]oleate and [^{3}H]cholesterol (or derived products), compared with control parasites. No significant difference was observed with respect to [^{14}C]palmitate internalization between the two parasite strains, which is in agreement with the lack of evidence for SCP-2b binding to palmitate (Figure 6). We next evaluated the contribution of each SCP-2 domain in the uptake of radioactive oleate or cholesterol, and in the synthesis of cholesteryl oleate and phospholipid from radioactive oleate (Table 1). For parasites expressing HA-TgSCP-2b or HA-TgSCP-2bΔSRL, we observed a significant increase in oleate uptake. However, HA-TgSCP-2b expressors also showed a higher incorporation of exogenous oleate in cholesteryl oleate and total phospholipids, compared with wild-type parasites. HA-TgSCP-2a expression did not result in increased lipid uptake although a significant stimulation in cholesteryl oleate synthesis was observed.

Finally, six mutant versions of TgSCP-2a and TgSCP-2b in which amino acids that are known to be important for lipid binding were engineered (Met345, Ile433, and Lys434 in SCP-2a and Met519, Leu608, and Lys609 in SCP-2b) to probe their roles in lipid interaction with parasite SCP-2 (Table 1). Results indicated that only HA-SCP-2b^{K609A} expressors were significantly impaired in the production of phospholipids and cholesteryl oleate, whereas the mutant parasites HA-SCP-2a^{M345K}, HA-SCP-2a^{I433K}, HA-TgSCP-2b^{M519k}, and HA-TgSCP-2b^{L608K} displayed the same ability in lipid acquisition and synthesis as parasites transfected with unaltered versions of TgSCP-2a or TgSCP-2b. This suggests that amino acids essential for lipid binding activity in mammalian SCP-2 may differ from that of parasite TgSCP-2 or that multiple mutations in the parasite SCP-2 are required to induce significant changes in the protein conformation.

Jointly, these observations suggest to some extent, selective roles for TgSCP-2a and TgSCP-2b domains in mediating the uptake of cholesterol and oleate into the parasites and redistributing of these lipids to lipid synthesis and storage sites.

DISCUSSION

Successful replication of *T. gondii* requires considerable amounts of lipids for membrane biogenesis. This parasite lacks the capacity to autonomously synthesize subsets of lipids, and instead scavenges the needed lipids from the host environment (reviewed in Coppens, 2006). Subsequent to diverting host lipid to the PV, *Toxoplasma* must be able to import these exogenous lipids from the plasma membrane and to distribute them to various compartments. In this

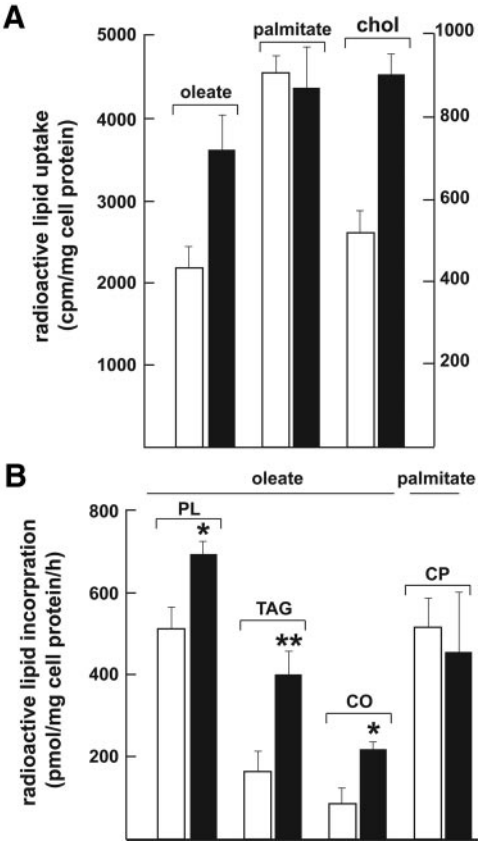

Figure 10. Contribution of TgHAD-2SCP-2 in lipid uptake and formation in *Toxoplasma*. (A) Lipid uptake assays. After infection with control *T. gondii* (white symbols) or parasites expressing HA-TgHAD-2SCP-2 (black symbols), fibroblasts were exposed to [^{14}C]oleate-BSA, [^{14}C]palmitate-BSA, or [^{3}H]cholesterol-LDL (chol) for 6 h at 37°C. After washing, parasites were isolated from host cells, and the amount of cell-associated lipids was determined by measuring radioactivity (expressed as cpm per milligram of cell protein). Data are means ± SD (n = 3), $p < 0.01$ for oleate and cholesterol uptake. (B) Lipid incorporation assays. Same parasite preparations and protocols were used as described in A except that the incubation time with [^{14}C]oleate-BSA or [^{14}C]palmitate-BSA was 60 min. After washing of infected cells and parasite purification, protein concentration was determined, and lipids were extracted to quantify the amount of radioactive phospholipids (PL), TAG, cholesteryl palmitate (CP), and cholesteryl oleate (CO) associated with the parasites. Values are means ± SD (n = 3 or 4). *$p < 0.05$ and **$p < 0.01$.

study, we reveal the role of a SCP-2 protein homologue for intracellular transportation, metabolism, and storage of host lipids in the parasite.

Toxoplasma SCP-2a and SCP-2b are members of the SCP-2 protein family. In contrast to many organisms, an SCP-2 in this parasite is not coded by a separate gene but is instead expressed in fusion with the enzyme D-3-hydroxyacyl-CoA dehydrogenase and a second SCP-2. Phylogenetic analysis reported that the multidomain TgHAD-2SCP-2 protein represents an alternative version of the large protein DBP, in which two enzymatic domains, D-3-hydroxyacyl-CoA dehydrogenase and enoyl-CoA hydratase are connected to a single SCP-2 domain (Edqvist and Blomqvist, 2006). In mammalian cells, the SCP-2 domain harbors a PTS1 and is responsible for the transport of DBP to peroxisomes (Gould *et al*., 1989). In peroxisomes, DBP undergoes proteolytic cleavage at a site between the two enzymatic domains. These domains take part in peroxisomal oxidation of fatty acids through D-3-hydroxyacyl-CoA intermediates. It is possible that SCP-2 facilitates these reaction cycles by providing lipid substrates to the enzymatic active sites.

The presence of HAD expressed in *Toxoplasma* is mystifying because integrated computational genomics ascertain the absence of functional pathways linked to fatty acid oxidation in this parasite. We showed that TgHAD-2SCP-2 is cleaved between the HAD domain and SCP-2a, and in the region between the two SCP-2 domains. After the TgHAD-2SCP-2 processing, the SCP-2 domains can potentially exert versatile cellular activities unrelated to fatty acid catabolism in *Toxoplasma*. From an evolutionary point of view, we speculate that if HAD is useless for the parasite, the presence of the *TgHAD-2SCP-2* gene in the *Toxoplasma* genome is more likely to reflect a need to retain the SCP-2 domain. A recent systematic investigation on the evolution of SCP-2 domains in eukaryotic organisms reveals indeed that over the course of evolution, *SCP-2* has been subjected to many genetic duplications, fissions, and fusions, from the point of its earliest appearance in the ancestral D-3-hydroxyacyl-CoA dehydrogenase/SCP-2 fusion (Edqvist and Blomqvist, 2006).

The majority of SCP-2 expressed in eukaryotic organisms harbor a PTS1 as found in peroxisomal matrix proteins. Likewise, the C-terminal −SRL of TgHAD-2SCP-2 matches the consensus of a PTS1, and we evidenced here that this motif represents a subcellular localization signal in the parasite. Shifting the PTS1 of TgHAD-2SCP-2 from the C terminus toward the center of TgHAD-2SCP-2 (in the Tg-HAD-2SCP-2-YFP construct) or deleting this motif from TgSCP-2b results in the cytosolic localization of the protein. This suggests that, like mammalian SCP-2, the C-terminal accessibility of TgHAD-2SCP-2 is critical for the interaction of −SRL with a receptor, and therefore the proper localization of the protein in the parasite.

In mammalian cells, the 58-kDa SCP-x protein is partially posttranslationally cleaved to a N-terminal 46-kDa protein (3-oxoacyl-CoA thiolase) and a C-terminal 13-kDa SCP-2 (Gallegos *et al*., 2001). So far, no information exists about the mechanism of cleavage—by autocatalysis or protease mediation—of mammalian SCP-2–containing proteins or about the cleavage site residues. The 58-kDa SCP-x is almost exclusively a peroxisomal protein and several observations support that posttranslational proteolysis of this protein occurs in peroxisomes either on the cytoplamic face of these organelles or inside their matrix. In view of that, Zellweger cells lacking peroxisomes express 58-kDa SCP-x but no 13-kDa SCP-2 can be detected. In most cells, 13-kDa SCP-2 has also a cytosolic localization, which implies that this domain cleaved from SCP-x must be leaked from the peroxosimes by an as yet unknown mechanism.

We have established that TgHAD-2SCP-2 undergoes at least two processing steps that occur simultaneously, which results in the release of an N-terminal 37-kDa HAD and two separate 13-kDa SCP-2 domains. Our data showed that TgHAD-2SCP-2 copurifies with parasite vesicles, indicating that after synthesis in the cytosol, the unprocessed protein is delivered to specific compartments, probably through the C-terminal −SRL motif. The lack of detection of any cleaved domains, HAD or SCP-2, on vesicles suggests either that these organelles, in contrast to mammalian peroxisomes, are maybe not the site of proteolytic cleavage of TgHAD-2SCP-2 or that partial cleavage of the protein may take place in vesicles but HAD and SCP-2 are rapidly transferred out of the vesicles to the cytosol. When parasites are transfected with a plasmid harboring the coding sequence of TgSCP-2b

Table 1. Comparison of lipid uptake and synthesis between wild-type parasites and transfectants

	Lipid uptake, cpm/mg cell protein (%)		Lipid synthesis, pmol/mg cell protein (%)	
	Oleate	Cholesterol	Cholesteryl oleate	Total phospholipids
Wild-type controls	1,990 ± 230 (100)	620 ± 155 (100)	133 ± 35 (100)	520 ± 40 (100)
HA-HAD-2SCP-2	3,382 ± 614 (170)**	811 ± 203 (131)*	223 ± 30 (168)*	777 ± 59 (149)*
HA-SCP-2a	2,355 ± 261 (118%)	750 ± 109 (121%)	194 ± 21(146%)	610 ± 33 (117%)
HA-SCP-2b	2,260 ± 305 (114)	841 ± 129 (135)*	242 ± 44 (182)**	692 ± 77 (133)*
HA-SCP-2bΔSRL	2,199 ± 100 (111)	789 ± 44 (127)*	155 ± 32 (116)	501 ± 58 (96)
HA-SCP-2a^{M345K}	2,444 ± 125 (123)	758 ± 59 (122)	199 ± 20 (150)*	690 ± 67 (133)*
HA-SCP-2b^{M519K}	2,985 ± 320 (150)*	730 ± 84 (118)	174 ± 32 (131)	622 ± 41 (117)
HA-SCP-2a^{I433K}	2,402 ± 365 (121)	745 ± 62 (120)	185 ± 40 (140)*	651 ± 77 (125)
HA-SCP-2b^{L608K}	2,807 ± 260 (141)*	699 ± 70 (113)	202 ± 39 (152)*	600 ± 34 (115)
HA-SCP-2a^{K434A}	1,699 ± 222 (85)	635 ± 124 (102)	104 ± 15 (78)	455 ± 62 (88)
HA-SCP-2b^{K609A}	2,003 ± 155 (101)	599 ± 62 (97)	99 ± 21 (74)*	378 ± 56 (73)*

Lipid uptake and incorporation assays are detailed in Figure 10 legend. Fibroblasts were infected with wild-type *T. gondii* or parasites expressing the indicated constructs before incubation with radioactive oleate or cholesterol to measure the uptake of these lipids, or with radioactive oleate to quantify the amount of radioactive cholesteryl oleate or total phospholipids synthesized by the parasites. Values are means ± SD (n = 3). *$p < 0.05$ and **$p < 0.01$.

alone and examined by IFA, immunoreactivity to this domain increases within vesicles over the cytoplasm. This suggests that once in the cytoplasm, SCP-2b may redistribute to vesicles, although the possibility that different populations of SCP-2–containing vesicles exist cannot be discounted.

The import of TgHAD-2SCP-2 into mammalian peroxisomes involves that the PTS1 present in the parasite sequence can interact with a mammalian PTS1 receptor. In mammalian cells, recognition of PTS1 is facilitated by the protein receptor peroxin 5 (PEX5), which cycles between the cytosol and peroxisomes in mammalian cells (Dodt and Gould, 1996). However, searches in the *T. gondii* EST database for PEX5 homologue was fruitless although putative PEX11, PEX7, and PEX1 could be retrieved by sequence homologies [expectation values from e^{-23} to e^{-56}]. Mammalian PEX7 is a cytosolic and peroxisomal receptor for peroxisomal proteins carrying a membrane PTS2 (mPTS2) at the N terminus, whereas PEX11 and PEX1 are required for peroxisome fusion/division (Titorenko and Rachubinski, 2001). Our data demonstrated that SCP-2 protein is membrane-bound in vesicles, suggesting that a PTS2 targeting pathway may be used by the protein though no conventional mPTS2 is detectable in the TgHAD-2SCP-2 sequence. In mammalian cells, SCP-2 has a primary localization to peroxisomes but can also be found on the cytosolic face of the ER or inside mitochondria (Gallegos *et al*., 2001), two organelles with lipid metabolic properties. The absence of SCP-2a or SCP-2b from parasite ER and mitochondria may reflect the limited capabilities of the parasite for lipid synthesis or processing.

Peroxisomes or microbody-like structures have never been unambiguously identified in *Toxoplasma* (Kaasch and Joiner, 2000; Ding *et al*., 2000). Given the detection in *T. gondii* of enzymes involved in the glyoxylate cycle, the presence of glyoxysome-like organelles, which house fatty acid conversion to succinate and ultimately to glucose, is plausible. Common enzymes for peroxisomes include catalase and peroxidase that are involved in the decomposition of hydrogen peroxide. Only catalase is present in the parasite. *Toxoplasma* catalase contains an atypical PTS1 but localizes to mammalian peroxisomes. One study illustrates that catalase is present primarily in punctate compartments anterior to the nucleus in *T. gondii*, which may correspond to peroxisomal structures (Kaasch and Joiner, 2000). Conversely, two other studies showed a cytosolic localization of GFP fused with the C-terminal 12 amino acids containing the putative PTS1 from *T. gondii* catalase or full-length catalase (Ding *et al*., 2000, 2004). A possible explanation for the results obtained by Ding and colleagues is that upstream sequence elements of catalase (beyond the C-terminal 12 amino acids) may modulate the targeting efficiency of catalase to parasite organelles. Indeed, PTS1 upstream sequences in many peroxisomal proteins contribute to the protein stability, carboxy-terminal accessibility or translocation into peroxisomes (Neuberger *et al*., 2004). It is known that *Toxoplasma* proteins contain evolutionarily conserved and unconventional targeting signals that direct proteins to specific organelles. Therefore, if *Toxoplasma* catalase is not associated with peroxisomal compartments despite the presence of a PTS1, the protein sequence may contain competing targeting signals that prevent the translocation of catalase into a compartment. An alternative hypothesis is that PTS1 motifs may have occurred as a result of neutral mutation during evolution. Indeed, organisms lacking peroxisomes such as bacteria express proteins that harbor a PTS1-like carboxy-terminal signal.

Peroxisomes are heterogeneous and dynamic organelles that differ in size (ranging in diameter from 0.1 to 1 μm), number and protein composition, depending on the organism, cell type, and environmental condition (Titorenko and Rachubinski, 2001). The characteristics of the parasite compartment containing TgHAD-2SCP-2 and cleaved products are compatible with the size of large spherical peroxisomes. Colocalization studies with peroxisomal markers would provide a definitive answer about the existence of a peroxisomal endomembrane system and functional PTS-like targeting pathways in *T. gondii*.

Of interest, parasites expressing exogenous copies of SCP-2 accumulate lipid bodies at the basal end. Compared with the apical end of the parasite, which contains specialized organelles with clearly defined localization, much less is known about the architecture, organization, and organelle composition of the basal end. Parasite division by endodyogeny, an internal budding process that creates two daughter cells inside the mother cell, seems to be coordinated at the basal end (Gubbels *et al*., 2006; Hu, 2008). Undeniably, this pole contains structural elements for daughter cell formation but how new membranous systems and organelles expand during progeny formation still re-

mains elusive. In this context, the *Toxoplasma* SCP-2 domains may primarily play a role in parasite replication by providing the needed lipids for organellar membrane biosynthesis. Lipid bodies in *Toxoplasma* contain large amounts of neutral lipids such as cholesteryl esters and triacylglycerols (Quittnat *et al*., 2004; Nishikawa *et al*., 2005), which are synthesized by the parasite. The enhancement of cholesterol and oleate uptake and their incorporation into neutral lipids in SCP-2 expressors may be concurrent with the local concentration of neutral lipid stores at the posterior end. We can assume that cholesteryl esters and triacylgycerols stored at this area of *T. gondii* may constitute energy sources or a ready source of the lipids required for endodyogeny. Interestingly, a role for SCP-2 in stimulating cholesteryl ester formation and regulating fatty acid and cholesterol targeting to lipid bodies has been reported in fibroblasts transfected with SCP-2 (Atshaves *et al*., 2001). SCP-2 expression in fibroblasts dramatically influences the composition of the core and surface lipids of lipid bodies. No changes in lipid body size and no SCP-2 interaction with lipid bodies have ever been observed upon parasite SCP-2 overexpression in *Toxoplasma* or fibroblasts.

Cholesterol originating from the host cell must be translocated across the plasma membrane of *T. gondii*. In mammalian cells, SCP-2 can transfer sterols from the plasma membrane to the cell interior (e.g., to ER and lipid bodies; Moncecchi *et al*., 1996; Atshaves *et al*., 2001). SCP-2 colocalizes with caveolin-1 at the plasma membrane, and together these proteins enhance cholesterol transfer (Atshaves *et al*., 2003; Zhou *et al*., 2004). In yeast, nonvesicular sterol trafficking from the plasma membrane to the ER involves oxysterol-binding protein-related proteins (ORPs; Raychaudhuri *et al*., 2006). The genome of *Toxoplasma* does not encode any *caveolin* genes. Our unpublished data on the characterization of an ORP2 homologue in the parasite localized the protein to the PV (Zhang, Lige, and Coppens, unpublished). Our immunogold EM studies do not detect SCP-2a or SCP-2b on the parasite surface though weak, transient interaction between SCP-2 and the plasma membrane may occur.

The lack of fatty acid-binding proteins (FABPs) in *Toxoplasma* may confer for the two parasite SCP-2, a FABP-like function in facilitating uptake, trafficking, and targeting of fatty acids. Parasite SCP-2 expression in mammalian cells results in enhancement of cholesterol transfer from the ER to the plasma membrane. Whether this movement of cholesterol from the ER to the parasite surface is operational in *T. gondii* remains to be demonstrated because no sterols are synthesized by *Toxoplasma* on the ER. Parasite SCP-2 also acts as a substrate carrier for phospholipids, shows weak affinity for ergosterol, and cannot bind to ceramide and palmitate. Ergosterol has not been detected in *Toxoplasma* (Nishikawa *et al*., 2005), but palmitate is the most abundant fatty acid found in cholesteryl esters, *n*-acylglycerides, and glycosylphosphatidylinositol anchors in the parasite (Coppens, 2006). Thus, alternative transport pathways must exist to facilitate palmitate trafficking in the parasite.

Among the large phylum of Apicomplexa, only *Eimeria tenella* has a predicted gene encoding a separate SCP-2 protein carrying a PTS1 (−SKL; Edqvist and Blomqvist, 2006). No *SCP-2*, fused or separate, has been found in the genome of *Plasmodium* or *Cryptosporidium* sp. *Toxoplasma* constitutes a unique example of a protozoan pathogen expressing a multidomain protein carrying two SCP-2 domains. In this study, we provide the first experimental evidence that the *Toxoplasma* SCP-2 homologue plays multiple roles in cholesterol, fatty acid, and phospholipid metabolism, intracellular transportation, and deposition into specific lipid pools. Our data underline, on one hand, the evolutionarily conservation of the mechanism of nonvesicular lipid movement mediated by SCP-2, and on the other hand, the exploitation of this lipid carrier by an intracellular parasite to enhance host lipid uptake and use.

ACKNOWLEDGMENTS

We thank Boris Striepen for thoughtful comments on the study. We also grateful to all members of the Coppens and Carruthers laboratories for helpful discussions during the course of this work. We are thankful to the Kimberly Zichichi at the Yale Center for Cell and Molecular Imaging for excellent assistance for electron microscopy. Support for this research was provided by National Institutes of Health grant AI-060767 and American Heart Association grants 0230079N and 0755368U.

REFERENCES

Altschul, S. F., Madden, T. L., Schäffer, A. A., Zhang, J., Zhang, Z., Miller, W., and Lipman, D. J. (1997). Gapped BLAST and PSI-BLAST: a new generation of protein database search programs. Nucleic Acids Res. *25*, 3389–3402.

Atshaves, B. P., Storey, S. M., McIntosh, A. L., Petrescu, A. D., Lyuksyutova, O. I., Greenberg, A. S., and Schroeder, F. (2001). Sterol carrier protein-2 expression modulates protein and lipid composition of lipid droplets. J. Biol. Chem. *276*, 25324–25335.

Atshaves, B. P., Gallegos, A. M., McIntosh, A. L., Kier, A. B., and Schroeder, F. (2003). Sterol carrier protein-2 selectively alters lipid composition and cholesterol dynamics of caveolae/lipid raft vs nonraft domains in L-cell fibroblast plasma membranes. Biochemistry *42*, 14583–14598.

Avdulov, N. A., Chochina, S. V., Igbavboa, U., Warden, C. S., Schroeder, F., and Wood, W. G. (1999). Lipid binding to sterol carrier protein-2 is inhibited by ethanol. Biochim. Biophys. Acta *1437*, 37–45.

Bradley, P. J., *et al*. (2005). Proteomic analysis of rhoptry organelles reveals many novel constituents for host-parasite interactions in *Toxoplasma gondii*. J. Biol. Chem. *280*, 34245–34258.

Brasaemle, D. L., and Attie, A. D. (1990). Rapid intracellular transport of LDL-derived cholesterol to the plasma membrane in cultured fibroblasts. J. Lipid Res. *31*, 103–112.

Choinowski, T., Hauser, H., and Piontek, K. (2000). Structure of sterol carrier protein 2 at 1.8 A resolution reveals a hydrophobic tunnel suitable for lipid binding. Biochemistry *39*, 1897–1902.

Coppens, I., Levade, T., and Courtoy, P. J. (1995). Host plasma low density lipoprotein particles as an essential source of lipids for the bloodstream forms of Trypanosoma brucei. J. Biol. Chem. *270*, 5736–5741.

Coppens, I., Sinai, A. P., and Joiner, K. A. (2000). Toxoplasma gondii exploits host low-density lipoprotein receptor-mediated endocytosis for cholesterol acquisition. J. Cell Biol. *149*, 167–180.

Coppens, I., and Joiner, K. A. (2003). Host but not parasite cholesterol controls *Toxoplasma* cell entry by modulating organelle discharge. Mol. Biol. Cell *14*, 3804–3820.

Coppens, I. (2006). Contribution of host lipids to *Toxoplasma* pathogenesis. Cell. Microbiol. *8*, 1–9.

Ding, M., Clayton, C., and Soldati, D. (2000). *Toxoplasma gondii* catalase: are there peroxisomes in *Toxoplasma*? J. Cell Sci. *113*, 2409–2419.

Ding, M., Kwok, L. Y., Schlüter, D., Clayton, C., and Soldati, D. (2004). The antioxidant systems in *Toxoplasma gondii* and the role of cytosolic catalase in defence against oxidative injury. Mol. Microbiol. *51*, 47–61.

Dodt, G., and Gould, S. J. (1996). Multiple PEX genes are required for proper subcellular distribution and stability of Pex5p, the PTS1 receptor: evidence that PTS1 protein import is mediated by a cycling receptor. J. Cell Biol. *135*, 1763–1774.

Dyer, D. H., Lovell, S., Thoden, J. B., Holden, H. M., Rayment, I., and Lan, Q. (2003). The structural determination of an insect sterol carrier protein-2 with a ligand-bound C16 fatty acid at 1.35-A resolution. J. Biol. Chem. *278*, 39085–39091.

Edqvist, J., Rönnberg, E., Rosenquist, S., Blomqvist, K., Viitanen, L., Salminen, T. A., Nylund, M., Tuuf, J., and Mattjus, P. (2004). Plants express a lipid transfer protein with high similarity to mammalian sterol carrier protein-2. J. Biol. Chem. *279*, 53544–53553.

Edqvist, J., and Blomqvist, K. (2006). Fusion and fission, the evolution of sterol carrier protein-2. J. Mol. Evol. *62*, 292–306.

Gallegos, A. M., Atshaves, B. P., Storey, S. M., Starodub, O., Petrescu, A. D., Huang, H., McIntosh, A. L., Martin, G. G., Chao, H., *et al*. (2001). Gene structure, intracellular localization, and functional roles of sterol carrier protein-2. Prog. Lipid Res. *40*, 498–563.

Gould, S. J., Keller, G. A., Hosken, N., Wilkinson, J., and Subramani, S. (1989). A conserved tripeptide sorts proteins to peroxisomes. J. Cell Biol. *108*, 1657–1664.

Gubbles, M. J., Vaishnava, S., Boot, N., Dubremetz, J. F., and Striepen, B. (2006). A MORN-repeat protein is a dynamic component of the Toxoplasma gondii cell division apparatus. J. Cell Sci. *119*, 2236–2245.

Hu, K. (2008). Organizational changes of the daughter basal complex during the parasite replication of *Toxoplasma gondii*. PLoS Pathog. *4*, e10.

Kaasch, A. J., and Joiner, K. A. (2000). Targeting and subcellular localization of *Toxoplasma gondii* catalase. Identification of peroxisomes in an apicomplexan parasite. J. Biol. Chem. *275*, 1112–1118.

Keller, G. A., Krisans, S., Gould, S. J., Sommer, J. M., Wang, C. C., Schliebs, W., Kunau, W., Brody, S., and Subramani, S. (1991). Evolutionary conservation of a microbody targeting signal that targets proteins to peroxisomes, glyoxysomes, and glycosomes. J. Cell Biol. *114*, 893–904.

Mattjus, P., Molotkovsky, J. G., Smaby, J. M., and Brown, R. E. (1999). A fluorescence resonance energy transfer approach for monitoring protein-mediated glycolipid transfer between vesicle membranes. Anal. Biochem. *268*, 297–304.

Moncecchi, D., Murphy, E. J., Prows, D. R., and Schroeder, F. (1996). Sterol carrier protein-2 expression in mouse L-cell fibroblasts alters cholesterol uptake. Biochim. Biophys. Acta *1302*, 110–116.

Mukherji, M., Kershaw, N. J., Schofield, C. J., Wierzbicki, A. S., and Lloyd, M. D. (2002). Utilization of sterol carrier protein-2 by phytanoyl-CoA 2-hydroxylase in the peroxisomal α oxidation of phytanic acid. Chem. Biol. *9*, 597–605.

Murphy, E. J. (2002). Sterol carrier protein-2, not just for cholesterol any more. Mol. Cell. Biochem. *239*, 87–93.

Neuberger, G., Kunze, M., Eisenhaber, F., Berger, J., Hartig, A., and Brocard, C. (2004). Hidden localization motifs: naturally occurring peroxisomal targeting signals in non-peroxisomal proteins. Genome Biol. *5*, R97.

Nishikawa, Y., Quittnat, F., Stedman, T. T., Voelker, D. R., Choi, J. Y., Zahn, M., Yang, M., Pypaert, M., Joiner, K. A., and Coppens, I. (2005). Host cell lipids control cholesteryl ester synthesis and storage in intracellular *Toxoplasma*. Cell Microbiol. *7*, 849–867.

Prinz, W. A. (2007). Non-vesicular sterol transport in cells. Prog. Lipid Res. *46*, 297–314.

Puglielli, L., Rigotti, A., Greco, A. V., Santos, M. J., and Nervi, F. (1995). Sterol carrier protein-2 is involved in cholesterol transfer from the endoplasmic reticulum to the plasma membrane in human fibroblasts. J. Biol. Chem. *270*, 18723–18726.

Quittnat, F. *et al*. (2004). On the biogenesis of lipid bodies in ancient eukaryotes: synthesis of triacylglycerols by a *Toxoplasma* DGAT1-related enzyme. Mol. Biochem. Parasitol. *138*, 107–122.

Raychaudhuri, S., Im, Y. J., Hurley, J. H., and Prinz, W. A. (2006). Nonvesicular sterol movement from plasma membrane to ER requires oxysterol-binding protein-related proteins and phosphoinositides. J. Cell Biol. *173*, 107–119.

Roos, D. S., Donald, R. G., Morrissette, N. S., and Moulton, A. L. (1994). Molecular tools for genetic dissection of the protozoan parasite *Toxoplasma gondii*. Methods Cell Biol. *45*, 27–63.

Sehgal, A., Bettiol, S., Pypaert, M., Wenk, M. R., Kaasch, A., Blader, I. J., Joiner, K. A., and Coppens, I. (2005). Peculiarities of host cholesterol transport to the unique intracellular vacuole containing *Toxoplasma*. Traffic *6*, 1125–1141.

Smith, P. K., Krohn, R. I., Hermanson, G. T., Mallia, A. K., Gartner, F. H., Provenzano, M. D., Fujimoto, E. K., Goeke, N. M., Olson, B. J., and Klenk, D. C. (1985). Measurement of protein using bicinchoninic acid. Anal. Biochem. *150*, 76–85.

Stolowich, N. J., Petrescu, A. D., Huang, H., Martin, G. G., Scott, A. I., and Schroeder, F. (2002). Sterol carrier protein-2, structure reveals function. Cell. Mol. Life Sci. *59*, 193–212.

Titorenko, V. I., and Rachubinski, R. A. (2001). The life cycle of the peroxisome. Nat. Rev. Mol. Cell Biol. *2*, 357–368.

Wenk, M. R. (2006). Lipidomics of host-pathogen interactions. FEBS Lett. *580*, 5541–5551.

Zhou, M., Parr, R. D., Petrescu, A. D., Payne, H. R., Atshaves, B. P., Kier, A. B., Ball, J. M., and Schroeder, F. (2004). Sterol carrier protein-2 directly interacts with caveolin-1 in vitro and in vivo. Biochemistry *43*, 7288–7306.